Light scattering by a fluid in a nonequilibrium steady state. II. Large gradients

T. R. Kirkpatrick* and E. G. D. Cohen
The Rockefeller University, New York, New York 10021

J. R. Dorfman
Institute for Physical Science and Technology, University of Maryland, College Park, Maryland 20742

(Received 24 February 1982)

The equations derived in the first paper of this series for the correlation functions of mass, momentum, and energy densities are solved for a fluid subject to a large temperature gradient. The shape and intensity of the Rayleigh line show deviations from equilibrium that are proportional to the square of the temperature gradient. The deviations of the intensity of each Brillouin line from its equilibrium value as a function of the temperature gradient is obtained for the optimal scattering geometry. The intensity of one of these two Brillouin lines shows a maximum or minimum as a function of the temperature gradient, depending on the sign of the temperature derivatives of the coefficient of sound attenuation and thermal conductivity and on the orientation of the momentum transfer between fluid and light with respect to the temperature gradient. Further, the difference in intensity of the two Brillouin lines is found to be about three times smaller than predicted by the linear theory, consistent with the experiments of Beysens *et al.* Since all these results are due to mode-coupling effects, an experimental verification would constitute the first observation of mode-coupling effects away from criticality. The connection between (a) the mode-coupling effects responsible for the changes in the intensities of the Rayleigh and Brillouin lines, (b) the long-time tail contributions to the transport coefficients, and (c) the nonexistence of a virial expansion of the transport coefficients is discussed.

I. INTRODUCTION

As pointed out in the previous paper,[1] hereafter denoted by II, the spectrum of the light scattered from a fluid in a nonequilibrium steady state due to a temperature gradient, exhibits an asymmetry of the two Brillouin lines. Since this effect is due to mode coupling, i.e., a coupling of two sound modes to the heat flux, it allows one, in principle, to detect mode-coupling effects in nonequilibrium fluids. In II, a linear theory was presented which only took into account small deviations from the equilibrium theory. In this paper, in order to treat effects large compared to the equilibrium results, we extend the calculations of II to fluids with larger thermal gradients. In fact, we are interested in the dynamical structure factor $S(\vec{R}_0,\vec{k},\omega)$ and the integrated intensities of the Rayleigh and the Brillouin lines $I^H(\vec{R}_0,\vec{k})$ and $I^\sigma(\vec{R}_0,\vec{k})$ ($\sigma=\pm1$; $\vec{R}_0$ is the center of the scattering volume) where $X^T=T^{-1}dT/dR_x$ and the wave number k are such that $c\,|X^T|/\Gamma_s k^2\approx 1$.[2]

We will find that the intensity of the central line $I^H(\vec{R}_0,\vec{k})$ is greatly enhanced when compared to its value $I^H_{eq}(k)$ in thermal equilibrium, an effect that should be easily observable. In addition, we will be able to compare our results for $I^\sigma(\vec{R}_0,\vec{k})$ with the experimental data obtained by Beysens *et al.*,[3] provided the neglect of finite-size effects due to the fluid container can be justified (cf. Sec. VI, subsection 13a).

As in II, we will formulate the calculation of $S(\vec{R}_0,\vec{k},\omega)$, $I^H(\vec{R}_0,\vec{k})$, and $I^\sigma(\vec{R}_0,\vec{k})$for large gradients in terms of the hydrodynamic modes associated with the matrix $\underline{H}_0(\vec{R},\vec{q})$. Therefore, in general, we write the dynamical structure factor as [cf. Eqs. (II.2.8) and (II.3.5a)]

$$S(\vec{R}_0,\vec{k},\omega)=2\,\mathrm{Re}\left[\int d\vec{R}\,P^2(\vec{R})\right]^{-2}\int d\vec{R}\,P^2(\vec{R})\int\frac{d\vec{q}}{(2\pi)^3}P^2_{\vec{k}-\vec{q}}[M_{H\rho}(\vec{R},\vec{q},\omega)+M_{+\rho}(\vec{R},\vec{q},\omega)+M_{-\rho}(\vec{R},\vec{q},\omega)]\,. \tag{1.1}$$

In Eq. (1.1) the $M_{a\rho}(\vec{R},\vec{q},\omega)$ ($a=H$, $\sigma=\pm 1$) are defined in terms of the $M_{\alpha\rho}(\vec{R},\vec{q},\omega)$ ($\alpha=\rho,\vec{g},\epsilon$) by Eq. (II.3.4). Furthermore, the total integrated intensity of all three spectral lines $I(\vec{R}_0,\vec{k})$ is given by [cf. Eqs. (II.4.4) and (II.4.5)]

$$I(\vec{R}_0,\vec{k})=I^H(\vec{R}_0,\vec{k})+I^+(\vec{R}_0,\vec{k})+I^-(\vec{R}_0,\vec{k}) \quad (1.2)$$

with

$$I^a(\vec{R}_0,\vec{k})=\mathrm{Re}\left[\int d\vec{R}\,P^2(\vec{R})\right]^{-2} \times\int d\vec{R}\,P^2(\vec{R}) \times\int\frac{d\vec{q}}{(2\pi)^3}P^2_{\vec{k}-\vec{q}}M_{a\rho}(\vec{R},\vec{q})\,, \quad (1.3)$$

where $a=H$ or σ.

In this paper we compute the line shape and the integrated intensity of the Rayleigh line and the integrated intensity of each Brillouin line. The shape of the Brillouin lines will not be computed inasmuch as the expansion parameters $c/\Gamma_s k^2 L$ and $L\mid\vec{\nabla}c\mid k/\Gamma_s k^2$ are large under the conditions we consider here.[2] As a consequence, these lines have a broad, flat shape which is not interesting, since it is due to the form factor $P(\vec{R})$ that describes the scattering volume, rather than to an intrinsic property of the fluid.

The plan of this paper is as follows. In Sec. II we use an ordering scheme to derive equations for the unequal- and equal-time correlation functions $M_{\alpha\rho}$ and $D_{\alpha\beta}$ from the basic equations (II.2.9) and (II.2.6), respectively, given in paper II. These equations are then solved to obtain the above-mentioned quantities in a consistent manner for the case $c\mid X^T\mid/\Gamma_s k^2$ is of $O(1)$.[4] In Sec. III we solve a set of algebraic equations needed for the calculation of the shape and intensity of the Rayleigh line. In Sec. IV the partial differential equation that determines the intensity of the two Brillouin lines is solved. In Sec. V the results obtained in this paper are used to compute $S^H(\vec{R}_0,\vec{k},\omega)$, $I^H(\vec{R}_0,\vec{k})$, and $I^\sigma(\vec{R}_0,\vec{k})$ for two fluids: water and liquid argon. In Sec. VI a final discussion of the results obtained in this and the preceding papers is given; in particular, a comparison with the available experimental data is made and some open questions are mentioned.

II. BASIC EQUATIONS FOR $M_{\alpha\rho}$ AND $D_{\alpha\beta}$

In paper II we derived equations for the quantities $M_{\alpha\rho}(\vec{R},\vec{q},\omega)$ and $D_{\alpha\beta}(\vec{R},\vec{q})$ under the conditions that $\Gamma_s q^2/cq\ll 1$ and $c\mid X^T\mid/\Gamma_s q^2\ll 1$. We now want to consider the case that $c\mid X^T\mid/\Gamma_s q^2\approx 1$ but we still require that $\Gamma_s q^2/cq\ll 1$ and, therefore, also $\mid X^T\mid/q\ll 1$. As mentioned in paper II, the condition $\Gamma_s q^2/cq\approx ql\ll 1$ is required so that a hydrodynamic description of the spatial variations of the $M_{\alpha\rho}$ and the $D_{\alpha\beta}$ is valid. In our analysis of the $M_{\alpha\rho}$ and $D_{\alpha\beta}$ here, we will keep terms of all orders in the parameter of order unity $c\mid X^T\mid/\Gamma_s q^2$, but in each order of X^T we will consistently neglect terms that are smaller than the leading term by factors of $\Gamma_s q^2/cq$. That is, we will only keep terms of order $(cX^T/\Gamma_s q^2)^n$ for all $n\geq 1$. Furthermore, we will assign a weight X^T to each derivative with respect to the center-of-mass position $\vec{R}=(\vec{R}_1+\vec{R}_2)/2$ and a weight q^0 to each term of the form $q(\partial/\partial q_x)$.[5]

A. Ordering scheme

Our procedure is to examine the hydrodynamic equations for the $M_{a\rho}(\vec{R},\vec{q},\omega)$ near $\omega=0$ for the shape of the Rayleigh line and those for $D_{\alpha\beta}(\vec{R},\vec{q})$ for the intensities of the Rayleigh and Brillouin lines, retaining at first all orders in $\vec{q}$ and X^T. We examine then the solutions of these equations obtained in the form of expansions in powers of $cX^T/\Gamma_s q^2$ with coefficients that depend on q and retain only the leading terms in each power of X^T as described above.

To carry out this procedure, we go back to II and examine the basic hydrodynamic matrix $\underline{\bar{H}}(\vec{R},\vec{q})$ that appears in the equations for $M_{\alpha\rho}(\vec{R},\vec{q},\omega)$ and $D_{\alpha\beta}(\vec{R},\vec{q})$. From Eqs. (II.2.9) and (II.2.6) these equations are

$$-i\omega M_{\alpha\rho}(\vec{R},\vec{q},\omega)=M_{\alpha\rho}(\vec{R},\vec{q},t=0) +\bar{H}_{\alpha\gamma}(\vec{R},\vec{q})M_{\gamma\rho}(\vec{R},\vec{q},\omega) \quad (2.1)$$

and[6]

$$\bar{H}_{\alpha\gamma}(\vec{R},\vec{q})D_{\gamma\beta}(\vec{R},\vec{q})+\bar{H}_{\beta\gamma}(\vec{R},-\vec{q})D_{\alpha\gamma}(\vec{R},\vec{q}) =(\delta a_{\alpha T}\delta a_{\beta T}S_{xT})_{0,\vec{R}}\beta X^T\,, \quad (2.2)$$

where Eq. (2.2) is a Fourier transform of Eq. (II.2.6). Next, we write the full matrix $\underline{\bar{H}}(\vec{R},\vec{q})$ with all powers of q and X^T retained as

$$\underline{\bar{H}}(\vec{R},\vec{q})=\underline{H}_0(\vec{R},\vec{q})+\Delta\underline{\bar{H}}(\vec{R},\vec{q})\,. \quad (2.3)$$

Here $\underline{\bar{H}}_0(\vec{R},\vec{q})$ is the linearized hydrodynamic ma-

trix whose elements are identical to the $\bar{H}_{\alpha\beta,0}$ defined in Eq. (II.2.12), and $\Delta\underline{\bar{H}}(\vec{R},\vec{q}) = \underline{\bar{H}}(\vec{R},\vec{q}) - \underline{\bar{H}}_0(\vec{R},\vec{q})$. By examining Eq. (II.2.12), we see that the matrix elements of $\underline{\bar{H}}_0$ are expansions in powers of q with coefficients that depend on the transport coefficients and thermodynamic quantities at the point $\vec{R}$. In Appendix A, we show that the matrix operator $\Delta\underline{H}(\vec{R},\vec{q})$ has the form

$$\Delta\underline{H}(\vec{R},\vec{q}) \approx X^T[O(1)+O(X^T/q)+O((X^T/q)^2)+\cdots][O(1)+O(lq)+O(lq)^2+\cdots], \tag{2.4}$$

where l is a microscopic correlation length, and that for $|X^T|/q \ll 1$ and $\Gamma_s q^2/cq \ll 1$, $\Delta\underline{\bar{H}}(\vec{R},\vec{q})$ need only be kept to $O(q^0X^T)$. To show this, one iterates Eqs. (2.1) and (2.2) and observes that the terms in $\Delta\underline{\bar{H}}(\vec{R},\vec{q})$ of $O(q^0X^T)$ are responsible for the most important contributions to $D_{\alpha\beta}$ and to $M_{\alpha\rho}[\vec{R},\vec{q},\omega \approx 0(q^2)]$ to every order in X^T (for small q) and properly take into account all terms of $O(1) \approx O((c|X^T|/\Gamma_s q^2)^n)$.

As a result of these considerations, we can replace $\Delta\underline{\bar{H}}(\vec{R},\vec{q})$ in Eqs. (2.1), (2.2), and (2.3) by the matrix $\Delta\underline{\bar{H}}_1^0(\vec{R},\vec{q})$ whose elements are given by

$$\Delta\bar{H}^0_{\rho\rho,1} = \Delta\bar{H}^0_{\rho\epsilon,1} = \Delta\bar{H}^0_{g_ig_j,1} = \Delta\bar{H}^0_{\epsilon\rho,1} = \Delta\bar{H}^0_{\epsilon\epsilon,1} = 0 , \tag{2.5a}$$

$$\Delta\bar{H}^0_{\rho g_i,1} = -\frac{\delta_{ix}}{2}\frac{\partial}{\partial R_x} , \tag{2.5b}$$

$$\Delta\bar{H}^0_{g_i\rho,1} = -\frac{A_1}{2}\delta_{ix}\frac{\partial}{\partial R_x} - \frac{1}{2}\frac{\partial A_1}{\partial R_x}\left[\delta_{ix} - q_i\frac{\partial}{\partial q_x}\right] , \tag{2.5c}$$

$$\Delta\bar{H}^0_{g_i\epsilon,1} = -\frac{A_2}{2}\delta_{ix}\frac{\partial}{\partial R_x} - \frac{1}{2}\frac{\partial A_2}{\partial R_x}\left[\delta_{ix} - q_i\frac{\partial}{\partial q_x}\right] , \tag{2.5d}$$

$$\Delta\bar{H}^0_{\epsilon g_i,1} = -\frac{A_3}{2}\delta_{ix}\frac{\partial}{\partial R_x} - \frac{1}{2}\frac{\partial A_3}{\partial R_x}\left[\delta_{ix} - q_i\frac{\partial}{\partial q_x}\right] . \tag{2.5e}$$

The quantities A_1, A_2, and A_3 in Eq. (2.5) have been defined below Eq. (II.2.13) and they all depend on the center-of-mass point $\vec{R}$. We remark that $\Delta\underline{\bar{H}}_1^0(\vec{R},\vec{q})$ is identical to the matrix $\Delta\underline{\bar{H}}_1(\vec{R},\vec{q})$, defined by Eqs. (II.2.13), if one neglects the elements in $\Delta\underline{\bar{H}}_1(\vec{R},\vec{q})$ of $O(qX^T)$ and $O(q^2X^T)$ and keeps only those of $O(q^0X^T)$.

B. Basic equations for $D_{\alpha\beta}$ and $M_{\alpha\rho}$

The basic equations for $D_{\alpha\beta}$ and $M_{\alpha\rho}$ are derived using the matrix $\underline{H}_1(\vec{R},\vec{q})$ defined by the Eqs. (II.2.12) and (2.5). We first derive the equations for the $D_{\alpha\beta}$.

(1) The equations that determine the $D_{\alpha\beta}$ are

$$\bar{H}_{\alpha\gamma,1}(\vec{R},\vec{q})D_{\gamma\beta}(\vec{R},\vec{q}) + \bar{H}_{\beta\gamma,1}(\vec{R},-\vec{q})D_{\alpha\gamma}(\vec{R},\vec{q}) = (\delta a_{\alpha T}\delta a_{\beta T}S_{xT})_{0,\vec{R}_1}\beta X^T \tag{2.6a}$$

with

$$\bar{H}_{\alpha\beta,1}(\vec{R},\vec{q}) = \bar{H}_{\alpha\beta,0}(\vec{R},\vec{q}) + \Delta\bar{H}^0_{\alpha\beta,1}(\vec{R},\vec{q}) . \tag{2.6b}$$

As in the previous paper, we find it convenient in solving these equations to express the $D_{\alpha\beta}$ in terms of the $D_{ab}(\vec{R},\vec{q})$ defined by Eqs. (II.3.15) and (II.3.16), where both a and b denote elements of the set (σ,H,η_i) with $\sigma = \pm 1$ and $i = 1,2$. To perform this transformation, we use the hydrodynamic eigenmodes discussed in Appendix A of II. That is, we use

$$D_{ab}(\vec{R},\vec{q}) = \theta^{L,\alpha}_{a,0}(\vec{R},\vec{q})\theta^{L,\beta}_{b,0}(\vec{R},\vec{q})D_{\alpha\beta}(\vec{R},\vec{q}) \tag{2.7}$$

and convert Eq. (2.6) for the $D_{\alpha\beta}$ into a set of equations for the D_{ab}. As follows from the ordering scheme, discussed in Appendix A of this paper, it is sufficient for the solution of Eq. (2.6) to use these lowest-order eigenfunctions of $\underline{H}_0$ as given by Eqs. (II.A7) and (II.A10).

From Eqs. (2.6) and (2.7), algebraic and differential equations for the $D_{ab}(\vec{R},\vec{q})$ can be derived. As in II, the dominant contributions to the D_{ab} will come, for small q, from those pairs (a,b) for which the sum of the eigenvalues $\omega_a + \omega_b$ is of $O(q^2)$. Furthermore, in deriving equations for the D_{ab} it is convenient to use a coordinate system for $\hat{q}$, $\hat{q}_\perp^{(1)}$, $\hat{q}_\perp^{(2)}$ such that $\hat{q}_{\perp x}^{(2)} = 0$, e.g.,

$$\hat{q} = (\hat{q}_x,\hat{q}_y,\hat{q}_z) , \tag{2.8a}$$

$$\hat{q}_\perp^{(1)}=\frac{(-\hat{q}_y^2-\hat{q}_z^2,\hat{q}_x\hat{q}_y,\hat{q}_x\hat{q}_z)}{(\hat{q}_y^2+\hat{q}_z^2)^{1/2}}\ , \tag{2.8b}$$

$$\hat{q}_\perp^{(2)}=\frac{(0,\hat{q}_z,\hat{q}_y)}{(\hat{q}_y^2+\hat{q}_z^2)^{1/2}}\ . \tag{2.8c}$$

Using this coordinate system, neglecting the D_{ab} with $\omega_a+\omega_b\approx 0(q)$, we find, after a long calculation, that the equations for the D_{ab} break up into two sets: (1) A coupled set of algebraic equations for D_{HH}, $D_{H\eta_1}$, $D_{\eta_1 H}$, and $D_{\eta_1\eta_1}$ and (2) A partial differential equation for $D_{\sigma-\sigma}$ ($\sigma=\pm 1$). The coupled algebraic equations are

$$2D_T q^2 D_{HH}-c\alpha_T\frac{\partial T}{\partial R_x}\hat{q}_{\perp x}^{(1)}(D_{H\eta_1}+D_{\eta_1 H})=-(\delta a_{H,\hat{q}}\delta a_{H,-\hat{q}}S_{xT})_{0,\vec{R}}\beta X^T\ , \tag{2.9a}$$

$$(\nu+D_T)q^2 D_{H\eta_1}-c\alpha_T\frac{\partial T}{\partial R_x}\hat{q}_{\perp x}^{(1)}D_{\eta_1\eta_1}=-(\delta a_{H,\hat{q}}\delta a_{\eta_1,-\hat{q}}S_{xT})_{0,\vec{R}}\beta X^T\ , \tag{2.9b}$$

$$(\nu+D_T)q^2 D_{\eta_1 H}-c\alpha_T\frac{\partial T}{\partial R_x}\hat{q}_{\perp x}^{(1)}D_{\eta_1\eta_1}=-(\delta a_{\eta_1,\hat{q}}\delta a_{H,-\hat{q}}S_{xT})_{0,\vec{R}}\beta X^T\ , \tag{2.9c}$$

and

$$2\nu q^2 D_{\eta_1\eta_1}=-(\delta a_{\eta_1,\hat{q}}\delta a_{\eta_1,-\hat{q}}S_{xT})_{0,\vec{R}}\beta X^T\ , \tag{2.9d}$$

while the partial differential equation for $D_{\sigma-\sigma}$ is

$$\left[\Gamma_s q^2-\sigma\frac{\partial c}{\partial R_x}q\frac{\partial}{\partial q_x}+\sigma\hat{q}_x c\frac{\partial}{\partial R_x}+\sigma\hat{q}_x cX^T-\sigma\hat{q}_x\frac{c^3}{\rho T}\left[\frac{\partial}{\partial R_x}\frac{\rho T}{c^2}\right]\right]D_{\sigma-\sigma}=-(\delta a_{\sigma,\hat{q}}\delta a_{-\sigma,-\hat{q}}S_{xT})_{0,\vec{R}}\beta X^T\ . \tag{2.10}$$

The mode-coupling amplitudes appearing on the right-hand side of Eqs. (2.9) and (2.10) can be computed without difficulty[7] and are given by

$$(\delta a_{H,\hat{q}}\delta a_{H,-\hat{q}}S_{xT})_{0,\vec{R}}=(\delta a_{\eta_1,\hat{q}}\delta a_{\eta_1,-\hat{q}}S_{xT})_{0,\vec{R}}=0\ , \tag{2.11a}$$

$$(\delta a_{\eta_1,\hat{q}}\delta a_{H,-\hat{q}}S_{xT})_{0,\vec{R}}=(\delta a_{H,\hat{q}}\delta a_{\eta_1,-\hat{q}}S_{xT})_{0,\vec{R}}=\frac{-\rho\alpha_T T\hat{q}_{\perp x}^{(1)}}{c\beta^2}\ , \tag{2.11b}$$

and

$$(\delta a_{\sigma,\hat{q}}\delta a_{-\sigma,-\hat{q}}S_{xT})_{0,\vec{R}}=\frac{\rho\sigma c\hat{q}_x}{2c^2\beta^2}\ . \tag{2.11c}$$

Equations (2.9), (2.10), and (2.11) are a set of algebraic and differential equations that determine the $D_{ab}(\vec{R},\vec{q})$. From these equations and Eqs. (II.2.4), (II.3.13), (II.3.15), and (II.3.16) the equal-time correlation functions $M_{a\rho}(\vec{R},\vec{q})$ can be obtained. We next consider equations for the $M_{a\rho}(\vec{R},\vec{q},\omega)$.

(2) From Eq. (2.1), the equations that determine the $M_{a\rho}$ in the approximation outlined above are

$$-i\omega M_{a\rho}(\vec{R},\vec{q},\omega)-\bar{H}_{a\gamma,1}(\vec{R},\vec{q})M_{\gamma\rho}(\vec{R},\vec{q},\omega)=M_{a\rho}(\vec{R},\vec{q})\ . \tag{2.12}$$

As in the case of the $D_{a\beta}$, it is convenient to express the $M_{a\rho}$ in terms of $M_{a\rho}(\vec{R},\vec{q},\omega)$ defined by Eq. (II.3.4). Multiplying Eq. (2.12) by $\sum_\alpha\theta_{a,0}^{L,\alpha}(\vec{R},\vec{q})$ and using Eq. (II.A11a) yields

$$[-i\omega+\omega_a(q)]M_{a\rho}(\vec{R},\vec{q},\omega)-\theta_{a,0}^{L,\alpha}(\vec{R},\vec{q})\Delta\bar{H}_{\alpha\gamma,1}^0(\vec{R},\vec{q})\times\theta_{a',0}^{R,\gamma}(\vec{R},\vec{q})M_{a'\rho}(\vec{R},\vec{q},\omega)=M_{a\rho}(\vec{R},\vec{q})\ . \tag{2.13}$$

Here we have defined $M_{a\rho}(\vec{R},\vec{q},\omega)$ and $M_{a\rho}(\vec{R},\vec{q})$ in terms of $M_{a\rho}(\vec{R},\vec{q},\omega)$ and $M_{a\rho}(\vec{R},\vec{q})$, respectively, by Eq. (II.A11e) and summation convention has been used.

From Eq. (2.13) we can then derive equations that determine

$$M_{\rho\rho}(\vec{R},\vec{q},\omega)=M_{H\rho}(\vec{R},\vec{q},\omega)+\sum_{\sigma=\pm}M_{\sigma\rho}(\vec{R},\vec{q},\omega)$$

near $\omega\approx 0$. These equations can be greatly simplified by using the estimates of $(-i\omega+\omega_a)^{-1}$, $\partial/\partial q_x(-i\omega+\omega_a)^{-1}$, and $\partial/\partial R_x(-i\omega+\omega_a)^{-1}$ near $\omega=0$ given in Appendix II B. From these estimates, we conclude that $M_{\sigma\rho}(\vec{R},\vec{q},\omega)$ can be neglected in Eqs. (1.1) and (2.13) if we are only interested in frequencies ω near zero. Then carrying out the implied sum in Eq. (2.13), using Eqs. (2.5) and (2.8), we obtain the following coupled equations

for $M_{H\rho}$ and $M_{\eta_1\rho}$:

$$(-i\omega+D_Tq^2)M_{H\rho}(\vec{R},\vec{q},\omega)+c\frac{\partial \ln\rho}{\partial R_x}\hat{q}^{(1)}_{\perp x}M_{\eta_1\rho}(\vec{R},\vec{q},\omega)=M_{H\rho}(\vec{R},\vec{q}) \tag{2.14a}$$

and

$$(-i\omega+\nu q^2)M_{\eta_1\rho}(\vec{R},\vec{q},\omega)=M_{\eta_1\rho}(\vec{R},\vec{q}) . \tag{2.14b}$$

Here

$$M_{H\rho}(\vec{R},\vec{q})=A_{H\rho}+D_{H\rho} \tag{2.15a}$$

and

$$M_{\eta_1\rho}(\vec{R},\vec{q})=A_{\eta_1\rho}+D_{\eta_1\rho} , \tag{2.15b}$$

where $A_{\eta_1\rho}=0$, $A_{H\rho}$ is given by Eq. (II.3.8), and $D_{\eta_1\rho}$ and $D_{H\rho}$ are determined by Eqs. (II.3.15), (II.3.16), and (2.9).

III. SHAPE AND INTENSITY OF THE CENTRAL LINE

In this section we use the results of Sec. II to compute the shape and intensity of the central line. From Eqs. (1.1) and (1.2) and that $M_{\sigma\rho}(\vec{R},\vec{q},\omega)$ can be neglected near $\omega=0$,[8] it follows that the line shape of the central line is given by

$$S^H(\vec{k},\omega)=2\,\mathrm{Re}\left[\int d\vec{R}\,P^2(\vec{R})\right]^{-2}\times\int d\vec{R}\,P^2(\vec{R})\int\frac{d\vec{q}}{(2\pi)^3}P^2_{\vec{k}-\vec{q}}\times M_{H\rho}(\vec{R},\vec{q},\omega) . \tag{3.1}$$

$M_{H\rho}(\vec{R},\vec{q},\omega)$ is obtained by solving Eqs. (2.9) and (2.14). The result is

$$M_{H\rho}(\vec{R},\vec{q})=\rho^2k_BT\chi_T\frac{(\gamma-1)}{\gamma}+\rho k_BT\frac{(\alpha_T\hat{q}^{(1)}_{\perp x}TX^T)^2}{D_T(\nu+D_T)q^4} \tag{3.2}$$

and

$$M_{H\rho}(\vec{R},\vec{q},\omega)=\left[\rho^2k_BT\chi_T\frac{(\gamma-1)}{\gamma}+\rho k_BT\frac{(\alpha_T\hat{q}^{(1)}_{\perp x}TX^T)^2}{D_T(\nu+D_T)q^4}\right](-i\omega+D_Tq^2)^{-1}+\rho k_BT\frac{(\hat{q}^{(1)}_{\perp x}\alpha_TTX^T)^2}{(\nu+D_T)(D_T-\nu)q^4}[(-i\omega+\nu q^2)^{-1}-(-i\omega+D_Tq^2)^{-1}] . \tag{3.3}$$

Inserting Eq. (3.3) into Eq. (3.1), we obtain an expression for $S^H(\vec{k},\omega)$ where both a center of mass and a $\vec{q}$ integral remain to be performed. If $kL\gg1$ and $L\,|X^T|\ll1$, as is the case in typical experiments,[9] we can expand $M_{H\rho}(\vec{R},\vec{q},\omega)$ about $M_{H\rho}(\vec{R}_0,\vec{k},\omega)$, where $\vec{R}_0$ is the location of the center of the scattering volume and neglect the corrections. With these approximations the resulting expression for $S^H(\vec{R}_0,\vec{k},\omega)$ is

$$S^H(\vec{R}_0,\vec{k},\omega)=\left[\rho^2k_BT\chi_T\left[\frac{\gamma-1}{\gamma}\right]+\rho k_BT\frac{(\alpha_T\hat{k}^{(1)}_{\perp x}TX^T)^2}{D_T(\nu+D_T)k^4}\right]\frac{2D_Tk^2}{\omega^2+(D_Tk^2)^2}+\rho k_BT\frac{(\hat{k}^{(1)}_{\perp x}\alpha_TTX^T)^2}{(D_T-\nu)(\nu+D_T)k^4}\left[\frac{2\nu k^2}{\omega^2+(\nu k^2)^2}-\frac{2D_Tk^2}{\omega^2+(D_Tk^2)^2}\right] \tag{3.4}$$

with $(\hat{k}^{(1)}_{\perp x})^2=\hat{k}_y^2+\hat{k}_z^2$ [cf. Eq. (2.8b)]. In Eq. (3.4) all quantities are to be evaluated at the center of the scattering volume $\vec{R}_0$. The integrated intensity of the central line is given by

$$I^H(\vec{R}_0,\vec{k})=\int_{-\infty}^{\infty}\frac{d\omega}{2\pi}S^H(\vec{R}_0,\vec{k},\omega)=\rho^2k_BT\chi_T\frac{(\gamma-1)}{\gamma}+\frac{\rho k_BT(\alpha_T\hat{k}^{(1)}_{\perp x}TX^T)^2}{D_T(\nu+D_T)k^4} . \tag{3.5}$$

Equation (3.5) follows directly from Eq. (3.2) and the relation

$$I^H(\vec{R}_0,\vec{k})=M_{H\rho}(\vec{R}_0,\vec{k})$$

for $kL\gg1$ and $L\,|X^T|\ll1$. We note that although all orders in X^T have been considered in the derivation of (3.5), the correction to the equilibrium result is only of order $(X^T)^2$. This is to be contrasted with the results for $I^\sigma(\vec{R}_0,\vec{k})$ for the Brillouin lines derived in Sec. IV [cf. Eqs. (4.14) and (4.21)], where all orders of X^T contribute. We postpone a

further discussion of these equations and their consequences until Secs. V and VI and turn our attention now to the calculation of the integrated intensities of the Brillouin lines $I^{\sigma}(\vec{R}_0,\vec{k})$.

IV. INTENSITIES OF THE BRILLOUIN LINES

To compute the intensities of the two Brillouin lines, we return to Eq. (2.10) and introduce the substitution

$$D_{\sigma-\sigma}(\vec{R},\vec{q})=\frac{\rho^2 k_B T\chi_T}{2\gamma}B^{\sigma}(\vec{R},\vec{q}) \tag{4.1}$$

which together with Eq. (2.11c) leads to the following equation for B^{σ}:

$$\left[\frac{\Gamma_s}{c}q^2-\frac{\sigma}{c}\frac{\partial c}{\partial R_x}q\frac{\partial}{\partial q_x}+\sigma\hat{q}_x X^T +\sigma\hat{q}_x\frac{\partial}{\partial R_x}\right]B^{\sigma}(\vec{R},\vec{q})=-\sigma\hat{q}_x X^T\,, \tag{4.2}$$

where we have used the identity $\chi_T=\gamma(\rho c^2)^{-1}$. In view of the q_x dependence of the terms in Eq. (4.2), it is convenient to introduce a spherical coordinate system with the x axis as the polar axis, such that $q_x=q\cos\theta$. Then defining $\mu=\cos\theta$, we obtain the equation

$$\left[\frac{\Gamma_s}{\mu c}q^2-\frac{\sigma}{c}\frac{\partial c}{\partial R_x}q\frac{\partial}{\partial q}-\frac{\sigma}{c}\frac{\partial c}{\partial R_x}\frac{(1-\mu^2)}{\mu}\frac{\partial}{\partial\mu} +\sigma X^T+\sigma\frac{\partial}{\partial R_x}\right]B^{\sigma}(R_x,q,\mu)=-X^T\sigma\,. \tag{4.3}$$

Equation (4.3) is a linear, first-order partial differential equation for $B^{\sigma}(R_x,q,\mu)$. Owing to some subtleties in its solution, to be discussed below, we have constructed solutions by two different methods. One method is to obtain an iterated solution in powers of $cX^T/\Gamma_s q^2$ presumably valid[10] for $c\,|X^T|/\Gamma_s q^2\ll 1$, and then extend the solution to the region where $c\,|X^T|/\Gamma_s q^2\approx 1$ by Borel summation techniques. The other method is to construct an explicit solution of Eq. (4.3) and to use as a boundary condition that the results of the previous paper should be recovered for small $|X^T|$. As each method has certain advantages, and as the analysis is rather delicate, we will present both methods, at least in outline. In this section we describe the differential equation method, while in Appendix B we outline the Borel summation technique. Both procedures lead to the same results.

We begin our analysis of Eq. (4.3) by noting that one can easily construct a solution in the form of a power series in X^T, by iterating about the zeroth-order solution

$$B_0^{\sigma}(R_x,q,\mu)=-\frac{\sigma X^T c\mu}{\Gamma_s q^2}\,. \tag{4.4}$$

By iterating Eq. (4.3), one can see that the spatial variation of only three physical quantities appear: the sound absorption coefficients $\Gamma_s(T(R_x))$; the coefficient of thermal conductivity $\lambda(T(R_x))$, through the dependence of dT/dR_x on position [cf. Eq. (4.6a)], and the velocity of sound $c(T(R_x))$. Since Γ_s is usually obtained from the sound attenuation coefficient $\alpha/f^2=2\pi^2\Gamma_s/c^3$, where f is the frequency of the sound wave, we will use $\alpha(T(R_x))$ instead of $\Gamma_s(T(R_x))$. We can express α λ, and c as functions of temperature alone since any density dependence can be eliminated by the condition that $\vec{\nabla}p=0$. Since the spatial variations of α, λ, and c depend on the particular fluid being studied, it is convenient to represent the temperature variation of these quantities at constant pressure in some general way with specific parameters that characterize the particular fluid. We shall consider two possible representations of the variation of α, λ, and c with temperature: (1) an exponential fit where $\alpha=\alpha_0 e^{m_1 T}$, $\lambda=\lambda_0 e^{m_2 T}$, and $c=c_0 e^{m_3 T}$ or (2) a power-law fit $\alpha=\alpha_1 T^{\delta_1}$, $\lambda=\lambda_1 T^{\delta_2}$, and $c=c_1 T^{\delta_3}$. Here α_0, λ_0, c_0, m_1, m_2, m_3, α_1, λ_1, c_1, and δ_1, δ_2, δ_3, are to be chosen to fit the experimental data for α, λ, and c for a particular fluid over the range of temperatures of interest here.

A. Case 1: Exponential fit

We shall do this by transforming Eq. (4.3), a partial differential equation, into an ordinary differential equation. Therefore, we introduce the following scaled variables:

$$B^{\sigma}(R_x,q,\mu)=F^{\sigma}(R_x,z_1,\mu)/T\,, \tag{4.5a}$$

where

$$z_1=\Gamma_s q^2\left[c\frac{\partial T}{\partial R_x}\right]^{-1}\,. \tag{4.5b}$$

Using the relations

$$\frac{\partial}{\partial R_x}\left[\lambda(T(R_x))\frac{\partial T(R_x)}{\partial R_x}\right]=0\,, \tag{4.6a}$$

i.e., Fourier's law, and

$$\frac{\partial}{\partial R_x}=\frac{\partial z_1}{\partial R_x}\frac{\partial}{\partial z_1}+\left.\frac{\partial}{\partial R_x}\right|_{\text{explicit}}\,, \tag{4.6b}$$

Eq. (4.3) becomes

$$\left[z_1+\sigma\mu(m_1+m_2)z_1\frac{\partial}{\partial z_1}-\sigma m_3(1-\mu^2)\frac{\partial}{\partial\mu}+\sigma\mu\left[\frac{\partial T}{\partial R_x}\right]^{-1}\frac{\partial}{\partial R_x}\bigg|_{\text{explicit}}\right]F^\sigma(R_{x_1},z_1,\mu)=-\sigma\mu\ . \tag{4.7}$$

Notice that all the explicit R_x dependence in the operator on the left hand side of Eq. (4.7) is contained in the term proportional to $\partial/\partial R_x)_{\text{explicit}}$. If we examine the iterated solution of this equation about $F^\sigma=-(\sigma\mu)/z_1$, we see that the term proportional to $\partial/\partial R_x)_{\text{explicit}}$ never contributes since it acts on functions of z_1 only. If then, the boundary condition also depends only on z_1 and μ and not explicitly on R_x, we can solve Eq. (4.7) by taking F^σ to be a function of z_1 and μ alone, and set $\partial/\partial R_x)_{\text{explicit}}F^\sigma=0$.[11] Thus, we consider the equation

$$\left[z_1+\sigma\mu(m_1+m_2)z_1\frac{\partial}{\partial z_1}-\sigma m_3(1-\mu^2)\frac{\partial}{\partial\mu}\right]F^\sigma(z_1,\mu)=-\sigma\mu\ . \tag{4.8}$$

A further simplification of this equation is possible if we take into account that experiments on Brillouin scattering with temperature gradients are most advantageous when the wave vector of the incident laser beam is perpendicular to the direction of the temperature gradient, and one looks at small-angle scattering. Then, if we note that $P_{\vec{k}-\vec{q}}$ in Eq. (1.3) is sharply peaked about $\vec{k}=\vec{q}$ if $kL\gg1$, and that if ψ is the scattering angle, we have $\mu=\cos\theta\cong\cos(\psi/2)$ (cf. Fig. 1), so that for this geometry $1-\mu^2=\sin^2\theta$ is very small.[12] Then Eq. (4.8) may be replaced by the equation[13]

$$\left[z_1+\sigma\mu(m_1+m_2)z_1\frac{\partial}{\partial z_1}\right]F^\sigma(z_1,\mu)=-\sigma\mu\ . \tag{4.9}$$

Since the quantity m_3 no longer appears in Eq. (4.9), it follows that for the scattering geometry considered here, the explicit variation of the sound velocity with temperature is not important.

Equation (4.9) is a first-order ordinary differential equation whose general solution is

$$F^\sigma(z_1,\mu)=F^\sigma(z_1^0)\exp\left[\frac{\sigma(z_1^0-z_1)}{[\mu(m_1+m_2)]}\right]-\frac{1}{(m_1+m_2)}\times\int_{z_1^0}^{z_1}\frac{dt}{t}\exp\left[\frac{\sigma(t-z_1)}{\mu(m_1+m_2)}\right], \tag{4.10}$$

where z_1^0 is some point where we know the value of F^σ. Because of the pole at $t=0$ in the integrand, $F^\sigma(z_1,\mu)$ will, in general, be a multivalued function in the complex z_1 plane. Therefore, we proceed by interpreting Eq. (4.9) as a differential equation in one of the cut complex planes illustrated in Fig. 2, so as to specify a particular branch of the function. We then impose the boundary conditions that F^σ vanishes at zero temperature gradient, i.e., that $F^\sigma(z_1^0,\mu)=0$ where $|z_1^0|=\infty$ and that the iterated solution of Eq. (4.9) be recovered if an asymptotic expansion of (4.10) is made for large z_1 (small tem-

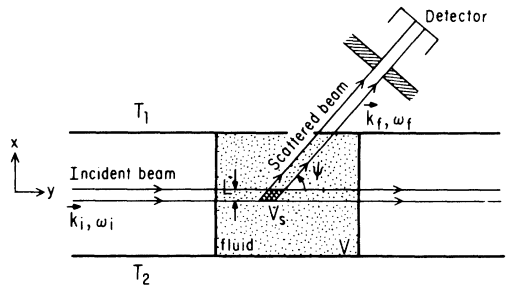

FIG. 1. Light-scattering experiment in the presence of a heat flux in the x direction. $\vec{k}_i$, ω_i and $\vec{k}_f$, ω_f are the wave numbers and frequency of the incident and scattered light waves, respectively. $\vec{k}=\vec{k}_f-\vec{k}_i$ and $\omega=\omega_f-\omega_i$ are proportional to the momentum and energy transfer from the fluid to the incident light wave. ψ is the scattering angle, V the volume of the fluid. V_s the scattering volume; T_1 and T_2 are the temperatures at the upper and lower walls of the fluid container, respectively.

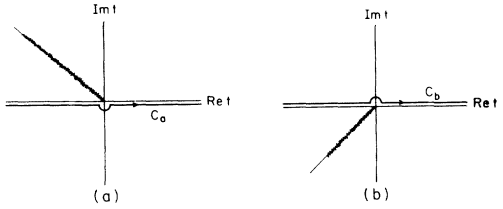

FIG. 2. C_a or C_b are two possible paths of integration for the t integrals in the cut complex t plane for the evaluation of the Eqs. (4.10) and (4.18) for the integrated intensities of the Brillouin lines. The latter are independent of which path (C_a or C_b) is chosen.

perature gradient). Then it follows that z_1^0 is given by

$$\frac{\sigma z_1^0}{\mu(m_1+m_2)} = -\infty \ . \tag{4.11}$$

The difference between the value of B^σ obtained by using either of the two contours illustrated in Fig. 2 is purely imaginary, and as only the real part of B^σ is of physical interest this nonuniqueness can be ignored. Thus, we can write

$$F^\sigma(z_1,\mu) = -\frac{1}{(m_1+m_2)} \times \int_{z_1^0}^{z_1} \frac{dt}{t} \exp\left[\frac{\sigma}{\mu(m_1+m_2)}(t-z_1)\right] . \tag{4.12}$$

Since only the real part of B^σ is needed, and returning to the original variables, we can express $B^\sigma(R_x,\vec{q})$ for $\mu \approx 1$, uniquely as

$$B_1^\sigma(R_x,\vec{q}) = -P\int_0^\infty dt\, e^{-t} \frac{\sigma c\hat{q}_x X^T}{[\Gamma_s q^2 - \sigma t c\hat{q}_x(m_1+m_2)TX^T]} , \tag{4.13}$$

where the subscript "1" denotes that an exponential fit for α and λ has been used and P denotes the principal part of the integral. The integrated intensity of the σ-Brillouin line $I_1^\sigma(\vec{R}_0,\vec{k})$ for this case is obtained by using Eqs. (1.2) and (1.3) together with Eqs. (4.1) and (4.13), and the relation [cf. Eq. (II.3.20)]

$$M_{\sigma\rho}(\vec{R},\vec{q}) = A_{\sigma\rho}(\vec{R},\vec{q}) + D_{\sigma-\sigma}(\vec{R},\vec{q})$$

which also holds here since the D_{ab} with $\omega_a+\omega_b \approx O(q)$ are smaller than the D_{ab} with $\omega_a+\omega_b \approx O(q^2)$ by factors $\sim \Gamma_s q^2/cq$. The result is then

$$I_1^\sigma(\vec{R}_0,\vec{k}) = \rho^2 \frac{k_B T}{2\gamma} \chi_T \left[1 - P\int_0^\infty dt\, e^{-t} \frac{\sigma c\hat{k}_x X^T}{[\Gamma_s k^2 - \sigma t c\hat{k}_x(m_1+m_2)TX^T]}\right] \tag{4.14}$$

provided $kL \gg 1$ and $L\,|X^T| \ll 1$, as is the case in typical experiments.[9] As before, all thermodynamic and hydrodynamic variables are to be evaluated at the center of the scattering volume $\vec{R}_0$. This result was first obtained by Kirkpatrick and Cohen[14] and it will be discussed in more detail in Sec. IV B.

B. Case 2: Power-law fit

An almost identical method can be used to treat the case where a power-law fit for the temperature dependence of α, λ, and c is used. Again we start from Eq. (4.3), introduce a new variable

$$z_2 = \Gamma_s q^2/cX^T = Tz_1 \tag{4.15}$$

to obtain the equation

$$\left[z_2 + \sigma\mu z_2 a\frac{\partial}{\partial z_2} - \sigma\delta_3(1-\mu^2)\frac{\partial}{\partial\mu} + \sigma\mu + \frac{\sigma\mu}{X^T}\frac{\partial}{\partial R_x}\bigg|_{\text{explicit}}\right] B_2^\sigma(R_x,z_2,\mu) = -\sigma\mu \ . \tag{4.16}$$

Here $a = 1+\delta_1+\delta_2$ and the subscript "2" denotes the power-law fit. Using similar arguments as before, we can eliminate the explicit dependence of B_2^σ on R_x, and for small scattering angles or for constant sound velocity, we can drop the term proportional to $\delta_3(1-\mu^2)$ on the left-hand side of Eq. (4.16). We then obtain the ordinary differential equation

$$\left[z_2 + \sigma\mu a z_2\frac{\partial}{\partial z_2} + \sigma\mu\right] B_2^\sigma(z_2,\mu) = -\sigma\mu \ , \tag{4.17}$$

the solution of which is given by

$$B_2^\sigma(z_2,\mu) = B_2^\sigma(z_2^0)\left[\frac{z_2^0}{z_2}\right]^{1/a} \exp\left[\frac{\sigma}{\mu a}(z_2^0-z_2)\right] - \frac{1}{a}\int_{z_2^0}^{z_2}\frac{dt}{t}\left[\frac{t}{z_2}\right]^{1/a}\exp\left[\frac{\sigma}{\mu a}(t-z_2)\right] . \tag{4.18}$$

Since the integral on the right-hand side of Eq. (4.18) may have poles and branch points at $t=0$, $B_2^\sigma(z_2)$ will, in general, be a multivalued function in the complex z_2 plane. Again we assume that $B_2^\sigma(z_2)$ vanishes at zero temperature gradient and we pick z_2^0 by a similar requirement as before, leading to

$$\frac{\sigma}{\mu a} z_2^0 = -\infty \ . \tag{4.19}$$

Then $B_2^\sigma(z_2)$ is given by

$$B_2^\sigma(z_2,\mu) = -\frac{1}{a}\int_{z_2^0}^{z_2} \frac{dt}{t}\left[\frac{t}{z_2}\right]^{1/a} \exp\left[\frac{\sigma}{\mu a}(t-z_2)\right], \qquad \frac{\sigma}{\mu a} z_2^0 = -\infty \tag{4.20}$$

where the path of integration in the t plane around the branch point at $t=0$ is illustrated in Fig. 2. If z_2 and $\sigma\mu a$ are both positive so that the integration does, in fact, go around the point at $t=0$, then the phase of t on the positive real axis must be chosen to be zero in order that the iterated solution of Eq. (4.17) is recovered for large z_2. As in case 1, the difference between the two contours of integrations in Fig. 2 is purely imaginary and, therefore, of no consequence to us here.

The integrated intensity of the σ-Brillouin line is then given by

$$I_2^\sigma(\vec{R}_0,\vec{k}) = \rho^2 \frac{k_B T \chi_T}{2\gamma}\left[1+\mathrm{Re}B_2^\sigma\left[z_2 = \frac{\Gamma_s k^2}{cX^T}\right]\right] \tag{4.21}$$

if $kL \gg 1$ and $L\,|X^T| \ll 1$. All thermodynamic and hydrodynamic quantities in Eq. (4.2) are to be evaluated at the center of the scattering volume $\vec{R}_0$. In Sec. V we will apply the results obtained here for $I^H(\vec{R}_0,\vec{k})$, $I_1^\sigma(\vec{R}_0,\vec{k})$, $I_2^\sigma(\vec{R}_0,\vec{k})$, and $S(\vec{R}_0,\vec{k},\omega\approx 0)$ to water and liquid argon.

V. RAYLEIGH AND BRILLOUIN LINES FOR H_2O and Ar

In this section we compute the shape and intensity of the Rayleigh line and the intensity of the Brillouin line for two liquids: water and argon, for several values of k and X^T. We will compare our results for the Brillouin lines with the recent experimental results obtained by Beysens, Zalczer, and Garrabos.[3]

A. Rayleigh line

In paper II we showed that the Rayleigh line is unaffected by the temperature gradient to linear order in the gradient. However, in Sec. III of this paper we obtained an effect of $O((X^T)^2)$ when higher-order terms in the gradient are taken into account and k is small, so that $(c_p/T)^{1/2}\,|X^T|/D_T k^2$ is of $O(1)$. A convenient quantity to graph in order to illustrate the shape of the central line is the reduced structure factor, defined by ($\Omega=\omega/D_T k^2$):

$$s^H(\vec{R}_0,\vec{k},\Omega) = \frac{S^H(\vec{R}_0,\vec{k},\omega) D_T k^2 \gamma}{\rho^2 k_B T \chi_T(\gamma-1)} \ . \tag{5.1}$$

With Eq. (3.4), we find that this quantity is given by

$$s^H(\vec{R}_0,\vec{k},\Omega) = \left[1+\frac{c_p}{T}\left[\frac{dT}{dR_x}\right]^2 \frac{(\hat{k}_y^2+\hat{k}_z^2)}{(\nu+D_T)D_T k^4}\right]\frac{2}{\Omega^2+1} + \frac{c_p}{T}\left[\frac{dT}{dR_x}\right]^2 \frac{(\hat{k}_y^2+\hat{k}_z^2)}{(D_T+\nu)(D_T-\nu)k^4}\left[\frac{2(\nu/D_T)}{\Omega^2+(\nu/D_T)^2} - \frac{2}{\Omega^2+1}\right], \tag{5.2}$$

where the equilibrium $s_{\mathrm{eq}}^H(k,\Omega)$ has the form

$$s_{\mathrm{eq}}^H(\vec{k},\Omega) = \frac{2}{\Omega^2+1} \ . \tag{5.3}$$

In deriving Eq. (5.2) we have used $\chi_T=\gamma/\rho c^2$ and $(\hat{k}_{\perp x}^{(1)})^2=\hat{k}_y^2+\hat{k}_z^2$ [cf. Eq. (2.8b)].

In Figs. 3 and 4 we have plotted $s^H(\mathrm{k},\Omega)$ for two different liquids, H_2O and Ar, respectively. In Fig. 3, we consider water at 1 atm and at a temperature of 20° C at the center of the scattering volume. s_{eq}^H represents the equilibrium value given by Eq. (5.3), s_1^H represents a plot of Eq. (5.2) for the case where $|dT/dR_x| = 75\mathrm{K\,cm^{-1}}$ and $k = 3\times 10^3\ \mathrm{cm^{-1}}$, while s_2^H represents the case where $|dT/dR_x| = 50\mathrm{K\,cm^{-1}}$ and $k = 2\times 10^3\ \mathrm{cm^{-1}}$. We have approximated $\hat{k}_y^2+\hat{k}_z^2$ by unity, corresponding

to the scattering geometry illustrated in Fig. 5(a), where $\vec{k}$ is perpendicular to the direction of the temperature gradient.

In Fig. 4, $s^H(\vec{k},\Omega)$ is plotted for liquid argon at a pressure of 60 atm, with a temperature of 110 K at the center of the scattering volume. Again, s^H_{eq} represents the equilibrium value while s^H_1 represents a plot of Eq. (5.2) where $|dT/dR_x| = 50\text{K cm}^{-1}$, $\hat{k}_y^2+\hat{k}_z^2=1$, and $k=3\times10^3\ \text{cm}^{-1}$.

B. The Brillouin lines

We introduce the reduced integrated intensity of the σ-Brillouin line i^σ by the equation

$$i^\sigma_{1,2}(\vec{R}_0,\vec{k})=\frac{I^\sigma_{1,2}(\vec{R}_0,\vec{k})}{I^\sigma_{eq}(\vec{R}_0,\vec{k})}\ . \tag{5.4}$$

Here the subscripts 1 or 2 denote, respectively, the exponential or power-law fit of the temperature dependence of α and λ, discussed in Sec. IV; $i^\sigma_1(\vec{R}_0,\vec{k})$ is given by Eq. (4.14) while $i^\sigma_2(\vec{R}_0,\vec{k})$ by Eq. (4.21). Furthermore, $I^\sigma_{eq}(\vec{R}_0,\vec{k})$ is given by Eq. (II.1.5a), with all thermodynamical properties taken at the position $\vec{R}_0$ (cf. the discussion at the end of paper II, Sec. III A.).

If $\hat{k}_x\dfrac{dT}{dR_x}>0$, then i^σ_1 can be easily transformed to

$$i^\sigma_1[\sigma(m_1+m_2)>0]=1-\frac{\sigma e^{-y_1}}{|m_1+m_2|\,T}\text{Ei}(y_1) \tag{5.5a}$$

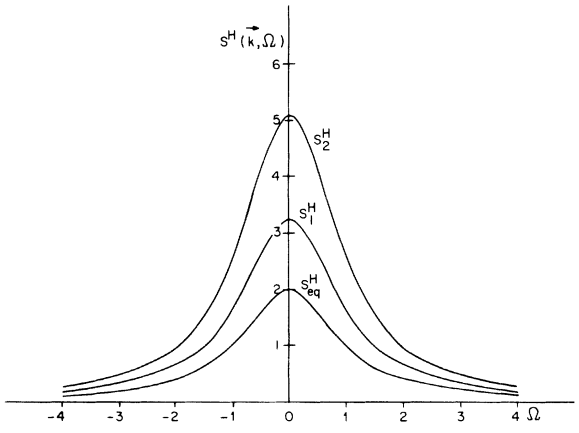

FIG. 3. Reduced structure factor of the Rayleigh line $s^H(\vec{R}_0,k,\Omega)$ of Eq. (5.2) as a function of $\Omega=\omega/D_Tk^2$ for water at 20°C and 1 atm for three cases: (1) s^H_1, $|dT/dR_x|=75$ K cm^{-1}, $k=3000$ cm^{-1}; (2) s^H_2, $|dT/dR_x|=50$ K cm^{-1}, $k=2000$ cm^{-1}; (3) s^H_{eq}, $|dT/dR_x|=0$.

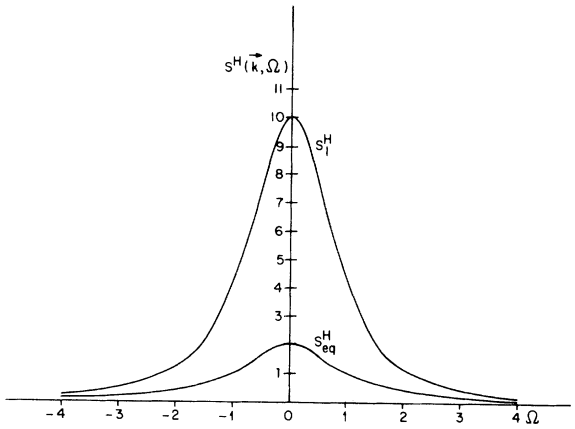

FIG. 4. Reduced structure factor of the Rayleigh line $s^H(\vec{R}_0,\vec{k},\Omega)$ of Eq. (5.2) as a function of $\Omega=\omega/D_Tk^2$ for liquid argon at 110 K and 60 atm for two cases: (1) s^H_1, $|dT/dR_x|=50$ K cm^{-1}, $k=3000$ cm^{-1}; (2) s^H_{eq}, $|dT/dR_x|=0$.

and

$$i^\sigma_1[\sigma(m_1+m_2)<0]=1-\frac{\sigma e^{y_1}}{|m_1+m_2|\,T}E_1(y_1)\ . \tag{5.5b}$$

Here y_1 is given by

$$y_1=\frac{\Gamma_s k^2}{c\,|m_1+m_2|\,\hat{k}_x\dfrac{dT}{dR_x}} \tag{5.6}$$

and $Ei(y_1)$ and $E_1(y_1)$ are exponential integrals defined by

$$\text{Ei}(y_1)=P\int_{-\infty}^{y_1}dt\frac{e^t}{t}\ , \tag{5.7a}$$

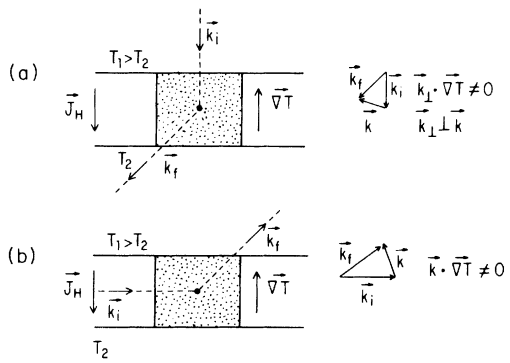

FIG. 5. Optimal geometry for light-scattering experiments to measure the change due to a temperature gradient (a) in the Rayleigh line and (b) the Brillouin lines. $\vec{J}_H$ is the heat flux and $\vec{\nabla}T$ the temperature gradient.

$$E_1(y_1)=\int_{y_1}^{\infty} dt\frac{e^{-t}}{t}\,, \tag{5.7b}$$

and conveniently tabulated by Abromowitz and Stegun.[15]

The reduced integrated intensity $i_2^{\sigma}(\vec{R}_0,\vec{k})$ is given by

$$i_2^{\sigma}(\vec{R}_0,\vec{k})=1+\mathrm{Re}B_2^{\sigma}(\vec{R},\vec{k})\,|_{\vec{R}=\vec{R}_0}\,, \tag{5.8}$$

where $B_2^{\sigma}(\vec{R},\vec{k})\,|_{\vec{R}=\vec{R}_0}$ is given by Eqs. (4.20) and (4.21), with $\vec{R}=\vec{R}_0$ and $\hat{k}_x\approx 1$. Thus, $i_2^{\sigma}(\vec{R}_0,\vec{k})$ can be evaluated when $a=1+\delta_1+\delta_2$ has been determined. These parameters δ_1, δ_2, a, as well as m_1 and m_2 needed for $i_{1,2}^{\sigma}$, were all determined by performing a least-squares fit to the experimental data for α and λ. The values obtained are listed in Table I.

In order to determine i_2^{σ}, we have used an absolutely convergent expansion of $B_2^{\sigma}(\vec{k})$, valid for $\hat{k}_x dT/dR_x>0$ and for $a=-6.025$, given by[16]

$$B^{+}\left[y_2=\frac{\Gamma_s k^2}{c\,|a|\,\hat{k}_x X^T}\right]=-1-y_2e^{y_2}\sum_{n=0}^{\infty}\frac{(-1)^n y_2^n}{n!\left[n+1-\frac{1}{|a|}\right]}+y_2^{1/|a|}e^{y_2}\Gamma\left[1-\frac{1}{|a|}\right] \tag{5.9a}$$

and

$$B^{-}\left[y_2=\frac{\Gamma_s k^2}{c\,|a|\,\hat{k}_x X^T}\right]=-1+y_2e^{-y_2}\sum_{n=0}^{\infty}\frac{y_2^n}{n!\left[n+1-\frac{1}{|a|}\right]}+\left[\cos\frac{\pi}{|a|}\right]y_2^{1/|a|}e^{-y_2}\Gamma\left[1-\frac{1}{|a|}\right]. \tag{5.9b}$$

In Fig. 6, the $i_{1,2}^{\sigma}(\vec{R}_0,\vec{k})$ are plotted for H_2O at 1 atm for a temperature of 40°C at the center of the scattering volume and for $\hat{k}_x(dT/dR_x)>0$. The straight line in the figure represents the value $i_0^{\sigma}=1-\sigma c\hat{k}_x X^T/\Gamma_s k^2$ given by Eq. (II.4.3a) and is the result of the linear theory discussed in II. In Fig. 7 we plot the quantities

$$\epsilon_{1,2}=(i_{1,2}^{+}-i_{1,2}^{-})/(i_{1,2}^{+}+i_{1,2}^{-})$$

for H_2O under the conditions listed above and compare these theoretical values with the experimental values for $\epsilon=(i^{+}-i^{-})/(i^{+}+i^{-})$ found by Beysens *et al.*[3] and with ϵ_0, the result of the linear theory.

In Fig. 8 we plot i_1^{σ} and i_0^{σ} for liquid Ar at 60 atm and with a temperature of 110 K at the center of the scattering volume. We do not give i_2^{σ} since the power-law fit does not represent the temperature variation of α and λ very well.

TABLE I. Sound damping (Γ_s), sound velocity (c), and the temperature variation of the sound attenuation and thermal conductivity in an exponential fit (m_1,m_2), or a power-law fit (δ_1,δ_2) to the experimental data, are listed in Table I for water at 40°C and 1 atm and liquid argon at 110 K and 60 atm.

	$10^2\Gamma_s$ (cm/sec)	$10^{-5}c$ (cm/sec)	m_1	m_2	δ_1	δ_2
H_2O	2.64	1.53	−0.0254	0.0025	−7.77	0.749
Ar	0.507	0.712	0.0259	−0.0123		

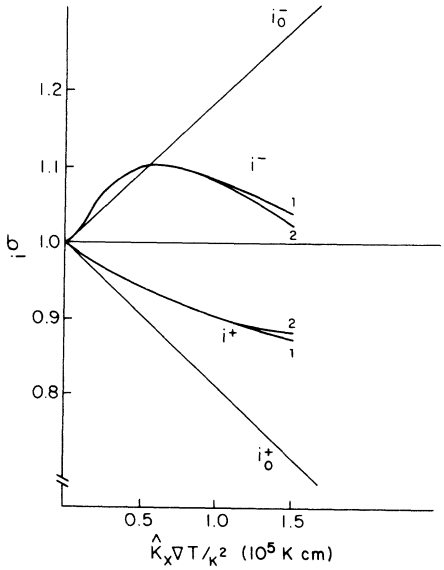

FIG. 6. Variation of the reduced integrated intensity i^{σ} of each of the Brillouin lines ($\sigma=\pm 1$) as a function of $\hat{k}_x\nabla T/k^2$ for water and for the case of an exponential (1) or a power-law (2) fit to the sound attenuation coefficient and the thermal conductivity. i_0^{σ} is the result of the linear theory discussed in the previous paper. Here $\nabla T\equiv dT/dR_x$.

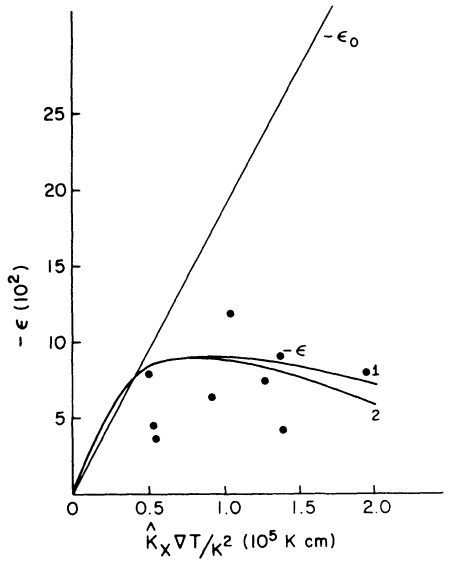

FIG. 7. Intensity difference of the two Brillouin lines $\epsilon=(i^+-i^-)/(i^++i^-)$ as a function of $\hat{k}_x\nabla T/k^2$ for water at 40°C. Straight line: linear theory ϵ_0; curved lines: large gradient theory, case 1, ϵ_1, and case 2, ϵ_2; dots: experiment.

VI. DISCUSSION

A number of comments on the results obtained in this paper will now be given. They are as follows.

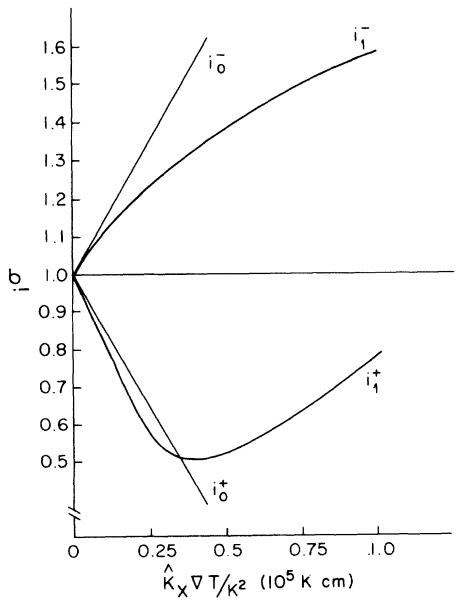

FIG. 8. Variation of the reduced integrated intensity i^σ of each of the Brillouin lines ($\sigma=\pm1$) as function of $\hat{k}_x\nabla T/k^2$ for liquid argon for case 1, i_1^σ, and the linear theory i_0^σ.

(1) The nonequilibrium contributions to the Rayleigh line, $s^H(\vec{R}_0,\vec{k},\Omega)$ as well as to $I^H(\vec{R}_0,\vec{k})$ are both proportional to $(\hat{k}_y^2+\hat{k}_z^2)(X^T)^2/k^4$. Thus, these corrections will be most important for small k and for scattering geometries where $\vec{k}$ is perpendicular to the temperature gradient.

(2) Both the height and the integrated intensity of the Rayleigh line are substantially increased by the presence of the temperature gradient. For experimentally realistic values of the temperature gradient (~75 K cm^{-1}) and for k (~2000 to 3000 cm^{-1}) these effects should be easily observable.

(3) We note that the effects of the thermal gradient on the Rayleigh line in liquid argon is considerably larger than in water. The same is true for the Brillouin lines. The reason for this is that since the hydrodynamic modes represent the lowest-lying excitations of a fluid, their importance increases when the (average) temperature of the fluid decreases.

(4) The integrated intensity of the Rayleigh line is determined by $M_{H\rho}(\vec{R},\vec{q})$, the Fourier transform of the equal-time correlation function $M_{H\rho}(\vec{R},\vec{R}_{12})$. The theory presented here for $M_{H\rho}(\vec{R},\vec{q})$ breaks down for sufficiently small q (i.e., when $|X^T|/q\approx1$) so that the asymptotic behavior of $M_{H\rho}(\vec{R},\vec{R}_{12})$ for large R_{12} cannot be determined. However, Eq. (3.5) does imply that for some intermediate range of values of R_{12},$M_{H\rho}(\vec{R},\vec{R}_{12})$ grows linearly with R_{12}.

(5) As in the linear theory discussed in paper II, the intensities of the Brillouin lines, i.e., the $B_{1,2}^\sigma$, like the B_0^σ defined by Eq. (4.4) and discussed in paper II, arise from a mode-coupling effect: the coupling of the two sound modes $(\sigma,\vec{k})$ and $(-\sigma,-\vec{k})$ to the heat flux. Similarly, the nonequilibrium contribution to the Rayleigh line $\sim(X^T)^2$ arises from the coupling of a viscous and a heat mode to the heat flux. Experimental verification, therefore, of either the increased intensity of the Rayleigh line or the predicted behavior of the Brillouin lines [cf. Appendix C below] in the presence of a thermal gradient would support the importance of mode-coupling effects in fluids not in equilibrium and away from a critical point.

(6) The extrema in $i_{1,2}^\sigma$ in Figs. 6 and 8 can be understood by examining, for example, the expression for i_1^σ given by the Eqs. (4.14) and (5.4):

$$i_1^\sigma=1-P\int_0^\infty dt\, e^{-t}\frac{\sigma c\hat{k}_x X^T}{[\Gamma_s k^2-\sigma tc\hat{k}_x(m_1+m_2)TX^T]}\,. \tag{6.1}$$

Now if $m_1+m_2<0$, as is the case for water, and if $\hat{k}_x(dT/dR_x)>0$, then for small gradients, both $i_1^+>i_0^+$ and $i_1^-<i_0^-$ as illustrated in Fig. 6. This can easily be seen by expanding in (6.1) about $(\Gamma_s k^2)^{-1}$. As the magnitude of the gradient increases—still with $\hat{k}_x(dT/dR_x)>0$— i_1^+ will continue to increase, but i_1^- will pass through a maximum before it will eventually decrease. For the case of liquid Ar, $m_1+m_2>0$ and then for $k_x(dT/dR_x)>0$, $i_1^+<i_0^+$, and $i_1^-<i_0^-$, i_1^+ has a minimum, while i_1^- continues to increase smoothly with increasing gradient. This dependence of the curves for $i_1^\pm$ on the sign of m_1+m_2 should provide a direct experimental test of the theory presented here.

(7) Since the integrated intensities of the Brillouin lines measure the sound-wave contributions to the equal-time correlation function, the second term in the denominator in Eq. (6.1) can be interpreted as an additional damping of this correlation function. This extra damping is caused by the coupling of two sound modes, characterized by $(\sigma,\vec{k})$ and $(-\sigma,-\vec{k})$ to the heat flux, thus allowing the temperature gradient to affect the $(\sigma,\vec{k})$ sound mode through the variation of its sound attenuation coefficient α, and the coefficient of thermal conductivity, λ with temperature. For sufficiently large gradients, this damping considerably reduces the contribution of B^σ to i^σ, so that $|i^\sigma|$ is much smaller than $|i_0^\sigma|$.

(8) In Fig. 7 we compared the theoretical results for water with the experimental data of Beysens *et al.*[3] Although their data points are of the same order of magnitude and have the same sign as our results, the scattering of their points prevents us from drawing any firm conclusion other than noting that a simple extrapolation of the small gradient theory to large gradients yields a result that is much too large. In addition, it is difficult to assess the role of boundary effects in the experiments of Beysens *et al.* where the cell size is roughly one-third of the mean-free path of the relevant sound wave of wave numbers $\vec{k}, c/\Gamma_s k^2$ [see point (13a) below].

(9) The integrated intensity of the Brillouin lines is proportional to the Fourier transform of the equal-time correlation function $M_{\sigma\rho}(\vec{R},\vec{R}_{12})$. As is the case for $M_{H\rho}(\vec{R},\vec{R}_{12})$, our theory cannot determine the asymptotically long-range behavior of $M_{\sigma\rho}(\vec{R},\vec{R}_{12})$, since $M_{\sigma\rho}(\vec{R},q)$ is not known for $q\lesssim|X^T|$. However, one can use $M_{\sigma\rho}(\vec{R},\vec{q})$ to show that for

$$R_{12}\ll[\Gamma_s/c\,|\,\vec{\nabla}T(m_1+m_2)\,|\,]^{1/2}$$

or $R_{12}\ll(\Gamma_s/\,c\,|\,a\vec{\nabla}T\,|\,)^{1/2}]$, $M_{\sigma\rho}(\vec{R},R_{12})$ is proportional to R_{12}^{-1}. For $R_{12}\gg[\Gamma_s/c|\vec{\nabla}T(m_1+m_2)|\,]^{1/2}$ one can obtain an estimate for the behavior of $M_{\sigma\rho}(\vec{R},\vec{R}_{12})$ by ignoring the angular dependence of $\hat{q}_x$ in $B^\sigma(R_x,\vec{q})$, i.e., by replacing $\hat{q}_x$ by unity and performing an inverse Fourier transform of $M_{\sigma\rho}(\vec{R},\vec{q})$. This leads to a behavior of $M_{\sigma\rho}\sim R_{12}^{-s}$, where s is of the order of 3. The correlation length $[\Gamma_s/c\,|\,\vec{\nabla}T(m_1+m_2)\,|\,]^{1/2}$ is of the order of 2.5×10^{-4} cm for H_2O at 40 K and $|\,\vec{\nabla}T\,|\approx75$ K cm^{-1}. The difference in behavior for large R_{12} of $M_{H\rho}$, discussed in point (4), and of $M_{\sigma\rho}$, discussed here, reflects the asymmetry introduced into the fluid by the thermal gradient.

(10) We have so far only discussed the case $\hat{k}_x dT/dR_x>0$. The values of i^σ and ϵ for $\hat{k}_x dT/dR_x<0$ can be obtained from the symmetry relation

$$B^\sigma\left[-\hat{k}_x\frac{dT}{dR_x}\right]=B^{-\sigma}\left[\hat{k}_x\frac{dT}{dR_x}\right]. \tag{6.2}$$

Equation (6.2) follows from Eq. (4.2) or also directly from the physics of the light-scattering experiment.

(11) In point (8), and point (13a) below, as well as in paper II, Appendix C, we discuss the possible effects of the boundaries on the intensities of the Brillouin lines in nonequilibrium fluids. There we note that for a complete theoretical discussion of the experiments by Beysens *et al.* one might need to include explicitly in the calculations the walls of the fluid container. Here we will suggest some experiments to measure the intensity of the Brillouin lines where the effects of the boundaries can be expected *a priori* to be small.

One possibility is to use the experimental geometry given in Fig. 5(a) to study the intensities of the Brillouin lines. In this geometry $\hat{k}_x\approx0$ so that the term linear in X^T in $I^\sigma(\vec{R}_0,\vec{k})$, vanishes. However, by iterating Eq. (4.2) for $B^\sigma(\vec{R},\vec{q})$ we see that the term of second order in X^T does not vanish as $\hat{k}_x\to0$. If $kL\gg1$ and $L\,|X^T|\ll1$ then from Eqs. (1.3), (II. 3.20), (4.1) and (4.2), the second-order result for $I^\sigma(\vec{R}_0,\vec{k})$ for small $\hat{k}_x$ is

$$I^\sigma(\vec{R}_0,k;\hat{k}_x\ll1)=\frac{\rho^2k_BT\chi_T}{2\gamma}\times\left[1-\left(\frac{cX^T}{\Gamma_sk^2}\right)^2\left(\frac{\partial\ln c}{\partial\ln T}\right)_p\right]. \tag{6.3}$$

The corrections to Eq. (6.3) near $\hat{k}_x \approx 0$ are of $O((cX^T/\Gamma_s k^2)^4)$, so that this equation can be used to predict small but detectable deviations from $I^{\sigma}_{\rm eq}(\vec{R}_0,\vec{k})$. We note, however, that there is no asymmetry of the Brillouin lines in Eq. (6.3) but an equal change in the intensity of both. For this geometry, the Brillouin lines are produced by sound waves that travel in a direction perpendicular to the temperature gradient, so that the finite-size effects should be minimized.

Another experiment that would minimize the effects of the walls is to use thermal gratings.[18] Here a temperature gradient is produced deep inside a fluid by the interference of two laser beams. Such experiments have been successfully carried out in a variety of systems[18] and might be useful here as well.

(12) In the course of this work we have mentioned the close connection between the dynamical processes responsible for the nonequilibrium contributions to the dynamical structure factor and those responsible for the long-time tails of the time-correlation functions that determine the transport coefficients as well as the appearance of logarithmic terms in the density expansions of the transport coefficients for moderately dense gases. We will sketch how these connections can be made in Appendix C for the case of a moderately dense gas, on the basis of kinetic theory so that a discussion of logarithmic terms in the density expansion of the transport coefficients can be included.

(13) Some open problems related to the research reported here are the following: (a) In all the calculations presented in this and the preceding paper, we have ignored effects due to the walls that surround the fluid. For the shape and intensity of the Rayleigh line the neglect of the walls can be justified by a calculation of Kirkpatrick and Cohen,[19] where the effects of the walls are explicitly taken into account. Since the results obtained with or without walls turn out to be identical, the effect of the walls can be neglected for the Rayleigh line.

For the Brillouin lines the situation is much less clear. Satten and Ronis,[20] using fluctuating hydrodynamics, have presented a calculation, where they find an important reduction of the intensity of the Brillouin lines, when the effects of the fluctuations of the fluid and the walls are explicitly taken into account. However, since they only treat the case of small gradients, i.e., $c\,|X^T|/\Gamma_s k^2 \ll 1$, the significance of the agreement of their results with the experiments of Beysens *et al.* is unclear, since in these experiments $c\,|X^T|/\Gamma_s k^2 \approx 1$ and a large gradient theory should be applied. Clearly, a theory that takes into account *both* wall effects and large gradients should be developed, but this has not been done so far. One might expect, though, that in such a theory the effects of the walls would be greatly reduced as compared to in a linear theory because of the strong extra damping of the sound modes due to the thermal gradient discussed above under point (4). This damping is taken into account only in a large gradient theory and is most effective when there is a large temperature dependence of α and λ.

(b) In this paper we used an infinite resummation technique to calculate the integrated intensities of the Brillouin lines for large thermal gradients. Although these results appear to be physically meaningful, the methods used to derive them could be criticized. For example, Fourier-transform methods were used for a spatially inhomogenous fluid which is unnatural and leads to a differential equation in wave-number space, without well-defined boundary conditions. An alternative method, using Borel summation and sketched in Appendix B gives results that are not necessarily unique. Thus, a better method to derive the above-mentioned results for the Brillouin lines is clearly indicated.

ACKNOWLEDGMENTS

The authors are much indebted to Dr. M. Arai, Dr. D. Beysens, Dr. H. Z. Cummins, Dr. J. Dufty, Dr. R. Gammon, Dr. E. H. Hauge, Dr. N. Khuri, Dr. J. Machta, Dr. I. Oppenheim, Dr. D. Ronis, and Dr. A. Tremblay for helpful discussions. This work was performed under National Science Foundation Contracts Nos. MCS80-17781 and CHE-77-16308.

APPENDIX A: ORDERING SCHEME FOR LARGE THERMAL GRADIENTS

I. Equations for the $D_{\alpha\beta}(\vec{R},\vec{q})$

In general, the $D_{\alpha\beta}(\vec{R},\vec{q})$ satisfy the Eq. (2.2) and the matrix $\underline{\overline{H}}(\vec{R},\vec{q})$ in Eq. (2.2) can be written in the form $\underline{\overline{H}}(\vec{R},\vec{q})=\underline{\overline{H}}_0(\vec{R},\vec{q})+\Delta\underline{\overline{H}}(\vec{R},\vec{q})$, where $\underline{\overline{H}}_0$ denotes the linearized hydrodynamic matrix given by Eq. (II. 2.12). The correction term $\Delta\underline{\overline{H}}$ is at least proportional to X^T, and one can show by explicit calculation (see below) that $\Delta\underline{\overline{H}}$ has the general structure of Eq. (2.4):

$$\Delta\underline{\overline{H}}(\vec{R},\vec{q}) \approx cX^T[1+O(X^T/q)+O(X^T/q)^2+\cdots] \times[1+O(lq)+O(l^2q^2)+\cdots], \quad \text{(A1)}$$

where l is a microscopic length.

To understand the form of Eq. (A1), we proceed as follows. Before we carry out a Fourier transform of the equation for $D_{\alpha\beta}(\vec{R}_1\vec{R}_2)$ with respect to their relative position $\vec{R}_{12}=\vec{R}_1-\vec{R}_2$, a typical (Euler) term on the left-hand side of Eq. (II. 2.6) is

$$\frac{\partial}{\partial R_{1x}} f(R_{1x}) D_{\alpha\beta}(\vec{R}_1,\vec{R}_2) , \tag{A2}$$

where $f(R_{1x})$ is some thermodynamic function that depends on R_{1x} [e.g., $c(R_{1x})$]. To carry out the Fourier transform of the above expression with respect to relative coordinates, we expand $f(R_{1x})$ around

$$f(R_x)=f(\tfrac{1}{2}(R_{1x}+R_{2x})) .$$

Doing this and using $\partial/\partial R_{1x}=\partial/\partial R_{12x}+\frac{1}{2}\partial/\partial R_x$, we find that the Fourier transform of Eq. (A2) has the form

$$\left[iq_x+\frac{1}{2}\frac{\partial}{\partial R_x}\right]\left[f(R_x)+\frac{df(R_x)}{dR_x}\frac{1}{2}\frac{\partial}{\partial iq_x}+\cdots\right]D_{\alpha\beta}(\vec{R},\vec{q})$$
$$=iq_x f(R_x)D_{\alpha\beta}(\vec{R},\vec{q})+X^T f(R_x)[1+O(X^T/q)+O(X^T/q)^2+\cdots]D_{\alpha\beta}(\vec{R},\vec{q}) , \tag{A3}$$

where we have used that $q\partial/\partial q_x \approx O(q^0)$ and $(1/f)df/dR_x \approx O(X^T)$. Examining Eqs. (A1) and (A3), we see that we have partially derived the general structure of $\Delta\underline{\bar{H}}(\vec{R},\vec{q})$. The remaining terms in (A1) arise from the Navier-Stokes terms in $\underline{\bar{H}}(\vec{R}_1)$ and can be obtained by similar arguments.

We next look for a solution of Eq. (2.2) in the form of an expansion in powers of X^T. The lowest-order solution is the one found in paper II and it satisfies the equation (II. 3.14):

$$\bar{H}_{\alpha\gamma,0}(\vec{R},\vec{q})D_{\gamma\beta,1}(\vec{R},\vec{q})+\bar{H}_{\beta\gamma,0}(\vec{R},-\vec{q})D_{\alpha\gamma,1}(\vec{R},\vec{q})$$
$$=(\delta a_{\alpha T}\delta a_{\beta T}s_{xT})_{0,\vec{R}}\beta X^T . \tag{A4}$$

In paper II we consistently retained only the contributions to $\underline{D}$, proportional to $cX^T/\Gamma_s q^2$, in our solution of (A4). Now we wish to consider the solution to Eq. (2.2) to all orders in X^T, so we expand the solution as

$$\underline{D}=\underline{D}_1+\underline{D}_2+\cdots \tag{A5}$$

where $\underline{D}_1$ satisfies Eq. (A4) and $\underline{D}_n$ satisfies the equation

$$\bar{H}_{\alpha\gamma,0}D_{\gamma\beta,n}+\bar{H}_{\beta\gamma,0}D_{\alpha\gamma,n}+\Delta\bar{H}_{\alpha\gamma}D_{\gamma\beta,n-1}$$
$$+\Delta\bar{H}_{\beta\gamma}D_{\alpha\gamma,n-1}=0 \tag{A6}$$

for $n\geq 2$. By expressing $\underline{D}_n$ in terms of eigenfunctions of $\underline{H}_0$ and selecting only combinations where

$$\bar{H}_{\alpha\gamma,0}D_{\gamma\beta,n}+\bar{H}_{\beta\gamma,0}D_{\alpha\gamma,n}\approx q^2 D_{\alpha\beta,n} ,$$

we see that $\underline{D}_1=0(X^T/q^2)$, and $\underline{D}_n=0((1/q^2)\times\Delta\underline{\bar{H}}D_{n-1})$. By examining the structure of $\Delta\underline{\bar{H}}$ given by Eq. (A1) we can see that the expansion (A5) of $\underline{D}$ in powers of X^T has the form

$$D=(X^T/q^2)[1+O(lq)]$$
$$+(X^T/q^2)^2[1+O(lq)]+\cdots$$
$$+(X^T/q^2)^n[1+O(lq)]+\cdots , \tag{A7}$$

where the leading term in the nth order of X^T has the form $(X^T/q^2)^n$, since q is sufficiently small that $lq\ll 1$. Furthermore, by combining Eqs. (A1), (A6), and (A7), we can see that the leading term in each order of X^T comes from the contribution to $\Delta\underline{\bar{H}}$ in (A1) that is of order cX^T. Consequently, if we restrict $\Delta\underline{\bar{H}}$ to terms of order q^0X^T, we will, upon solving Eq. (2.2), obtain an expression for D where all orders in X^T/q^2 have been summed together.

Finally, we point out that one can consistently use the lowest-order hydrodynamic modes when transforming the Eq. (2.6) for the $D_{\alpha\beta}$ to set of equations for the D_{ab}. This follows from the fact that the higher-order hydrodynamic modes lead to terms $\sim qD_{\alpha\beta}$ that are of higher order in q than need be retained. These considerations lead to Eq. (2.9) for D_{HH} and Eq. (2.10) for $D_{\sigma-\sigma}$.

II. Equation for $M_{\alpha\beta}(\vec{R},\vec{q},\omega)$ for large gradients

In order to determine the equation for the $M_{\alpha\rho}(\vec{R},\vec{q},\omega)$ when $c\,|X^T|/\Gamma_s q^2=0(1)$, $cq\gg\Gamma_s q^2$, and $\omega=0(q^2)$ we apply similar arguments as given above to the equation for $M_{\alpha\beta}(\vec{R},\vec{q},\omega)$ given by Eq. (2.1). Again, we decompose $\underline{\bar{H}}$ into $\underline{\bar{H}}_0+\Delta\underline{\bar{H}}$, where $\Delta\underline{\bar{H}}$ has the structure given by Eq. (A1). Since ω is also of order q^2, the leading contribution to $M_{\alpha\rho}$ in

each order of X^T will be of the form $(X^T/q^2)^n$, and $\Delta\underline{\bar{H}}$ can again be restricted to the order (q^0X^T). This argument leads to Eq. (2.14a) for $M_{H\rho}(\vec{R},\vec{q},\omega)$.

APPENDIX B: SOLUTION OF EQ. (4.3) BY BOREL SUMMATION

In this appendix we outline the solutions of Eq. (4.3) for the quantities $B^\sigma(R_x,q,\mu)$ that determine the integrated intensities of the Brillouin lines, obtained by the technique of Borel summation of a series. The essential steps of our application of the Borel summation method are as follows. We construct a solution of Eq. (4.3) as a power series in $cX^T/\Gamma_s q^2$. As we shall see, this series is asymptotic rather than convergent, even if $c\,|X^T|/\Gamma_s q^2 \ll 1$. However, this series can be formally summed by the method of Borel. We then analytically continue the resummed expression into the region where $c\,|X^T|/\Gamma_s q^2 \approx 1$, and take this result to be the value of $B^\sigma(R_x,q,\mu)$ for $c\,|X^T|/\Gamma_s q^2 \approx 1$. The results obtained by this procedure agree with those presented in Sec. IV, where we constructed solutions of Eq. (4.3) by quadratures.

For simplicity we consider here only the case of the exponential fit of the temperature dependence of α, λ, c, and we also make the small angle approximation that $\mu^2=\cos^2\theta\approx 1$. Then Eq. (4.3) for $B^\sigma(R_x,q,\mu)$ can be transformed to Eq. (4.9) for $F^\sigma(z_1,\mu)$, given by

$$\left[z_1+\sigma\mu(m_1+m_2)z_1\frac{\partial}{\partial z_1}\right]F^\sigma(z_1,\mu)=-\sigma\mu\ , \quad \text{(B1)}$$

where $B^\sigma(R_x,q,\mu)=F^\sigma(R_x,z_1,\mu)/T$ with $z_1=\Gamma_s q^2 \times[c(dT/dR_x)]^{-1}$. We expand the solutions of Eq. (B1) in powers of z_1^{-1}, which is equivalent to an expansion in powers of $cX^T/\Gamma_s q^2$ and find that

$$F^\sigma(z_1,\mu)=-\sum_{n=0}^{\infty}\frac{(\sigma\mu)^{n+1}(m_1+m_2)^n}{z_1^{n+1}}n!\ . \quad \text{(B2)}$$

Since a factor of $n!$ appears in the numerator, the series is asymptotic rather than convergent, for any value of z_1. The Borel method for summing the series is to write

$$n!=\Gamma(n+1)=\int_0^\infty dt\, t^n e^{-t}$$

and then to interchange the integration and summation. That is, we write

$$F^\sigma(z_1,\mu)=-\sum_{n=0}^{\infty}\frac{(\sigma\mu)^{n+1}(m_1+m_2)^n}{z_1^{n+1}}\int_0^\infty dt\, t^n e^{-t}$$
$$=-\int_0^\infty dt\frac{\sigma\mu}{z_1}\left[1-\frac{\sigma\mu(m_1+m_2)t}{z_1}\right]^{-1}e^{-t}\ . \quad \text{(B3)}$$

To be explicit, we consider the case where the fluid is H_2O, for which $m_1+m_2=-0.023$, and we suppose that $\mu(dT/dR_x)>0$. Then, we can write for $|\mu|\approx 1$:

$$B^\sigma(R_x,q,\mu)=\frac{-\sigma}{|m_1+m_2|\,Ty}\int_0^\infty dt\, e^{-t}\left[1+\frac{\sigma t}{y}\right]^{-1}, \quad \text{(B4)}$$

where $y=z_1[\mu\,|m_1+m_2|\,]^{-1}$. The integral on the right-hand side of Eq. (B4) is only well defined for $\sigma=\pm 1$. We first analyze this case and then show how $B^-(R_x,q,\mu)$ can be obtained by analytic continuation of the result obtained below for B^+.

For the case where $\sigma=+1$, the integral on the right-hand side of Eq. (B4) can be transformed by the substitution $t=yt'-y$, and $B^+(R_x,q,\mu)$ becomes for $|\mu|\approx 1$:

$$B^+(R_x,q,\mu)=-\frac{e^y}{|m_1+m_2|\,T}\int_1^\infty dt\frac{e^{-yt}}{t}$$
$$=-\frac{e^y}{|m_1+m_2|\,T}E_1(y)\ . \quad \text{(B5)}$$

Here $E_1(y)$ is defined by Eq. (5.7b). Equation (B5) is the first result of the Borel summation procedure. We have summed an alternating asymptotic series for $B^+(R_x,q,\mu)$ so as to obtain a result, Equation (B5) has an absolutely convergent expansion in powers of y (Ref. 17) given by

$$B^+(R_x,q,\mu)=\frac{1}{|m_1+m_2|\,T}e^y \times\left[\gamma+\ln y+\sum_{n=1}^{\infty}\frac{(-1)^n y^t}{n!}\right], \quad \text{(B6)}$$

where γ is Euler's constant.

To obtain $B^-(R_x,q,\mu)$ for the case where $y>0$, we can no longer use Eq. (B4) since the integrand on the right-hand side of Eq. (B4) has a pole at $t=y$ if $\sigma=-1$. Instead, we use Eq. (6.2), and that $B^+(R_x,q,\mu)$ given by Eq. (B6), defines a single-valued analytic function in a cut complex y plane. Thus, if we place the cut in the third quadrant of the y plane as illustrated in Fig. 2(b), we can define $B^+(R_x,q,\mu)$ for $\mu<0$, $|\mu|\approx 1$, as

$$B^{+}(R_x,q,-|\mu|)=\frac{1}{|m_1+m_2|T}e^{-|y|}\times\left[\gamma+\ln(-|\mu|)+\sum_{n=1}^{\infty}\frac{|y|^n}{n!}\right], \tag{B7}$$

where we take the principal branch of $\ln(-|y|)$ as $\ln(-|y|)=\ln|y|\pm i\pi$. We then obtain ($|\mu|\approx 1$):

$$\begin{aligned}\mathrm{Re}B^{-}(R_x,q,-|\mu|)&=\frac{e^{-|y|}}{|m_1+m_2|T}\times\left[\gamma+\ln|y|+\sum_{n=1}^{\infty}\frac{|y|^n}{n!}\right]\\&=\frac{e^{-|y|}}{|m_1+m_2|T}\mathrm{Ei}(|y|)\end{aligned} \tag{B8}$$

where $\mathrm{Ei}(y)$ is defined by Eq. (5.7a). Combining Eqs. (6.2) and (B8), we obtain

$$B^{-}(R_x,q,\mu)=\frac{e^{-y}}{|m_1+m_2|T}\mathrm{Ei}(y) \tag{B9}$$

for $y>0$. One can easily check that the results given by Eqs. (B5) and (B9) agree with those given by Eqs. (5.5a) and (5.5b), obtained by quadratures from the differential equation (4.9). The case where $\mu(dT/dR_x)<0$ or where the power-law fit of α, λ, and c is used, can be treated in a similar manner.

APPENDIX C: CONNECTION WITH LONG-TIME TAILS AND VIRIAL EXPANSION

In this appendix we shall demonstrate that the same mode-coupling effects that give rise to the enhanced intensity of the Rayleigh line and to the difference in intensity of the Brillouin lines also appear in the long-time tail contributions to the transport coefficients. Furthermore, we will show that these mode-coupling effects and the divergences that lead to the nonexistence of a virial expansion of the transport coefficients of a fluid are both related to the nonequilibrium part of the pair-correlation function $G_2(1,2)$ as defined by Eq. (I. 3.10).

We will discuss these connections on the basis of kinetic theory since then the light scattering, the long-time tails, and the nonexistence of a density expansion of the transport coefficients can all be treated from a single point of view.

The increased intensity of the Rayleigh line as well as the asymmetry in the intensities of the Brillouin lines are due to mode-coupling contributions to the pair-correlation function $G_2(1,2)$. The quantities that determine the nonequilibrium part of the intensities of the Brillouin lines are the $D_{\alpha\beta}(\vec{R},\vec{q})$ that are for low densities given directly in terms of $G_2(1,2)$ by Eq. (I. 3.7b) as

$$D_{\alpha\beta}(\vec{R},\vec{q})=\int d\vec{R}_{12}e^{-i\vec{q}\cdot R_{12}}\times\int d\vec{V}_1\int d\vec{V}_2 a_\alpha(\vec{V}_1)a_\beta(\vec{V}_2)\times G_2(1,2)\,, \tag{C1}$$

where the $a_\alpha(\vec{V}_1)$ are given by Eqs. (I. 2.9a)–(I.2.9c).

For low densities and for interparticle separations, R_{12}, greater than the range of the forces, i.e., for $R_{12}>\sigma$, $G_2(1,2)$ satisfies the equation (I. 3.10),

$$[L(1)+L(2)]G_2(1,2)=\hat{T}(12)F_1(1)F_1(2)\,, \tag{C2}$$

where $\hat{T}(12)$ is the binary-collision operator defined by Eq. (I. 2.13b) and the streaming operators $L(i)$ ($i=1,2$) are defined by Eq. (I. 2.34). In paper I, Sec. III, we showed that the hydrodynamic equations that determine the $D_{\alpha\beta}(\vec{R},\vec{q})$ follow directly from Eq. (C2) by considering the projection of G_2 onto the subspace spanned by products of hydrodynamic modes.

The connection between light scattering and the long-time tails is made by computing the thermal conductivity λ for a gas in a nonequilibrium steady state with a constant temperature gradient and demonstrating that (mode-coupling) contributions to λ exist that are determined by the $D_{\alpha\beta}$. As the computation of λ is rather long and has been carried out in detail by Ernst and Dorfman,[21] we merely outline the main results.

Ernst and Dorfman used Eq. (C2) to close the first hierarchy equation in the BBGKY hierarchy of equations for the distribution functions.[22] On the basis of the resulting equation for the single-particle distribution function one can obtain an expression for the thermal conductivity λ. The correction λ_R to the Boltzmann equation result λ_B for λ is then given by

$$\begin{aligned}\lambda_R=k_B\int d\vec{V}_1\int d\vec{V}_2\int\frac{d\vec{q}}{(2\pi)^3}V_{1x}\left[\frac{\beta m V_1^2}{2}-\frac{5}{2}\right]\frac{1}{\Lambda_l(1)}T_0(12)[i\vec{q}\cdot\vec{V}_{12}-\Lambda_l(1)-\Lambda_l(2)]^{-1}T_0(12)\\\times(1+P_{12})\frac{1}{\Lambda_l(1)}V_{1x}\left[\frac{\beta m V_1^2}{2}-\frac{5}{2}\right]F_l(1)F_l(2)\,,\end{aligned} \tag{C3}$$

where Λ_l and $T_0(12)$ in Eq. (C3) are defined by Eq. (I. 2.22) and by

$$\hat{T}(1,2)=\delta(\vec{R}_{12})T_0(1,2)$$

respectively. To evaluate λ_R, we divide the $\vec{q}$ integral in Eq. (C3) into two regions $0<q<q_0$ and $q_0<q<\infty$, where q_0^{-1} is on the order of a mean-free path l and treat each region separately.

(a) First we consider the region $0<q<q_0$.[24] For q in this range we can expand the operator $[\ ]^{-1}$ in terms of the eigenfunctions $\theta_a(\pm\vec{q},\vec{V}_i)$ and eigenvalues $\omega_a(q)$ of the operators $[\pm i\vec{q}\cdot\vec{V}_i-\Lambda_l(i)]$. One can see immediately on inspection of the right-hand side of Eq. (C3) that the most singular contribution to the $\vec{q}$ integral will come from those combinations of eigenfunctions $\theta_a(\vec{q},\vec{V}_1)$ and $\theta_b(-\vec{q},\vec{V}_2)$ with $[\omega_a(q)+\omega_b(q)]\to 0$ as $q\to 0$. These eigenmodes of $\pm i\vec{q}\cdot\vec{V}-\Lambda_l$, whose eigenvalues approach zero for $q\to 0$, are the kinetic counterparts of the five hydrodynamic modes discussed in Appendix A of paper II. For the eigenfunctions we refer to the literature,[21] but the corresponding eigenvalues $\omega_a(q)$ are given in paper II by Eqs. (II. A4b), (II. A7a), and (II. A8a) with all transport coefficients and thermodynamic quantities replaced by their low-density values. The contributions of the hydrodynamic modes to λ_R, denoted by $\lambda_R^{(H)}$, have the form

$$\lambda_R^{(H)}=k_B\sum_{a,b}{}'\int d\vec{V}_1\int d\vec{V}_2\int{}'\frac{d\vec{q}}{(2\pi)^3}V_{1x}\left[\frac{\beta m V_1^2}{2}-\frac{5}{2}\right]\frac{1}{\Lambda_l}T_0(12)\theta_a(\vec{q},\vec{V}_1)\theta_b(-\vec{q},\vec{V}_2)$$

$$\times F_l(1)F_l(2)D_{ab,1}(\vec{R},\vec{q})(X^T)^{-1}\ , \tag{C4}$$

where the summation over a and b runs only over the above-mentioned five hydrodynamic modes and the integral over $\vec{q}$ only over $0<q<q_0$ as indicated by the primes. The quantity $D_{ab,1}(\vec{R},\vec{q})$ is given by

$$D_{ab,1}(\vec{R},\vec{q})=[\omega_a(q)+\omega_b(q)]^{-1}\int d\vec{V}_1\int d\vec{V}_2\theta_a(\vec{q},\vec{V}_1)\theta_b(-\vec{q},\vec{V}_2)T_0(12)(1+P_{12})\frac{1}{\Lambda_l(1)}V_{1x}$$

$$\times\left[\frac{mV_1^2}{2}-\frac{5}{2\beta}\right]F_l(1)F_l(2)(\beta X^T)\ . \tag{C5}$$

The correspondence in notation between the $D_{ab,1}(\vec{R},\vec{q})$ defined by Eq. (C5) and the quantity $D_{ab,1}(\vec{R},\vec{q})$ appearing in Eqs. (II. 3.15) and (II. 3.16) is not accidental: One can verify that for low densities the two quantities are identical for a proper choice of the normalization of the hydrodynamic eigenfunctions. Therefore, the $D_{ab,1}$ that determine the integrated intensity of the Brillouin lines in light-scattering experiments is identical to the $D_{ab,1}$ that determine the mode-coupling contribution to the thermal conductivity. In order to make the connection with the long-time tail contributions to λ, we note that the $D_{ab,1}$, in λ_R with $\omega_a(q)+\omega_b(q)=O(q^2)$ will give a q dependence in the integrand of $\lambda_R^{(H)}$ proportional to q^{-2} [cf. Eqs. (II. 3.17)]. In particular, we consider the contribution of $D_{\sigma-\sigma}$ to $\lambda_R^{(H)}$.[25] $D_{\sigma-\sigma}$ determines the asymmetry of the intensities of the Brillouin lines and also leads to a contribution to $\lambda_R^{(H)}$ of the form

$$\lambda_R^{(H)}\sim\int_{q<q_0}\frac{d\vec{q}}{(2\pi)^3}\frac{1}{\Gamma_s q^2}\ , \tag{C6}$$

where $(\Gamma_s q^2)^{-1}$ in the integrand comes from the combination of eigenvalues $\omega_\sigma(q)+\omega_{-\sigma}(q)$. Integrals of this form lead directly to the sound-mode contributions to the long-time tails of the time-correlation functions $\rho_\lambda(t)$ that determine λ.[24] For, remembering that λ is a time integral over $\rho_\lambda(t)$, and writing

$$\int_{q<q_0}\frac{d\vec{q}}{(2\pi)^3}\frac{1}{\Gamma_s q^2}=\int_0^\infty dt\int_{q<q_0}\frac{d\vec{q}}{(2\pi)^3}e^{-\Gamma_s q^2 t}$$

$$\approx\int_{t>(cq_0)^{-1}}dt\,t^{-3/2}\ , \tag{C7}$$

we have

$$\rho_\lambda(t)\sim t^{-3/2}\ . \tag{C8}$$

That is, the q^2 denominators in λ_R are responsible for the $t^{-3/2}$ contribution, i.e., the long-time tail contribution to the time-correlation function $\rho_\lambda(t)$.

Thus, the two sound modes $(\sigma,\vec{q})$ and $(-\sigma,-\vec{q})$ that cause the difference in intensity of the two Brillouin lines in the presence of a temperature gradient, also contribute to the thermal conductivity λ through $\lambda_R^{(H)}$, with $a=\sigma,\vec{q}$; $b=-\sigma,-\vec{q}$. Physical-

ly, this follows immediately from the fact that the sound modes moving with the temperature gradient have larger amplitudes than those moving in the opposite direction, since this implies a contribution of the sound modes to the transport of heat in the fluid.

We note that the long-time tail contribution to the heat flux involves an integral over all q ($q<q_0$) of pairs of sound modes, while in a particular light-scattering experiment only one particular $\vec{q}\approx\vec{k}$ occurs.

(b) Next we consider the region $q_0<q$. The contribution from this region to λ_R, denoted by $\lambda_R^>$ is given by[26]

$$\lambda_R^> = k_B\int_0^\infty dt\int d\vec{V}_1\int d\vec{V}_2\int_{q>q_0}\frac{d\vec{q}}{(2\pi)^3}V_{1x}\left[\frac{\beta m V_1^2}{2}-\frac{5}{2}\right]\frac{1}{\Lambda_l(1)}T_0(12)$$
$$\times\exp\{-[i\vec{q}\cdot\vec{V}_{12}-\Lambda_l(1)-\Lambda_l(2)]t\}T_0(12)(1+P_{12})$$
$$\times\frac{1}{\Lambda_l(1)}V_{1x}\left[\frac{\beta m V_1^2}{2}-\frac{5}{2}\right]F_l(1)F_l(2)\,. \tag{C9}$$

In general, $\lambda_R^>$ is extremely difficult to compute because many of the spectral properties of the operator $[i\vec{q}\cdot\vec{V}_{12}-\Lambda_l(1)-\Lambda_l(2)]$ are not known for $q>q_0$. One possible way to evaluate Eq. (C9) is to assume that $\lambda_R^>$ has a power-series expansion in the density and expand

$$\exp-[i\vec{q}\cdot\vec{V}_{12}-\Lambda_l(1)-\Lambda_l(2)]t$$

in powers of $[\Lambda_l(1)+\Lambda_l(2)]$ since $\Lambda_l(i)$ is of $O(n)$ [cf. Eqs. (I. 2.19) and (I. 2.22)]. Phase-space estimates[27] and detailed calculations,[28] however, indicate that although the first two terms in this power-series expansion exist, the remaining terms are all divergent, with the strength of this divergence increasing with every term. These divergences are due to, for example, recollisions between the same two particles, where after their first collision each of these particles suffers a number of intermediate collisions with other particles before a second collision between them occurs. Since the time between the first and second collision of the two particles can be arbitrarily long, divergent integrals appear, the first of which is of the form

$$\lim_{T\to\infty}(n\sigma^3)^2\int_{t_\sigma}^T dt/t=\lim_{T\to\infty}(n\sigma^3)^2\ln T/t_\sigma\,,$$

where t_σ is the average time it takes for a particle to traverse a molecular diameter. As a consequence, $\lambda_R^>$ does not have a power-series expansion in the density, i.e., the transport coefficients do not have a virial expansion. To obtain convergent integrals, the exponential to Eq. (C9) should not be expanded in powers of $[\Lambda_l(1)+\Lambda_l(2)]$, but some aspect of these binary-collision operators must be retained in order to provide a cutoff for the time integrals, leading then to a cutoff on the time scale of the mean-free time $\tau\sim(n\sigma^2)^{-1}$. This in turn implies a nonanalytic expansion of $\lambda_R^>$, i.e., of λ in the density, since then a contribution of the form

$$(n\sigma^3)^2\ln\tau/t_\sigma\sim(n\sigma^3)^2\ln(n\sigma^3)$$

will arise. Thus, the nonexistence of a density expansion of the transport coefficients, the long-time tails, and the light-scattering phenomena discussed in these papers are all related to $G_2(1,2)$ through the $\vec{q}$ integral (C4) occurring in λ_R, albeit to different aspects of this integral.

---

*Present address: Institute for Physical Science and Technology, University of Maryland, College Park, Maryland 20742.

[1]T. R. Kirkpatrick, E. G. D. Cohen, and J. R. Dorfman, Phys. Rev. A 26, 972 (1982), preceding paper.

[2]For water and experimentally realistic values of $k\approx2000$ cm^{-1}, $T\sim313$ K, $|\vec{\nabla}T|\approx75$ K cm, $L=0.02$ cm, $c=1.53\times10^5$ cm/sec, and $\Gamma_s=2.62\times10^{-2}$ cm^2/sec, one has $c\,|X^T|/\Gamma_s k^2=0.35$, $c/\Gamma_s k^2 L\approx73$, and $L\,|\vec{\nabla}c\,|\,k/\Gamma_s k^2\approx14$. Here L is the linear dimension of the scattering volume in the direction of the temperature gradient.

[3]D. Beysens, Y. Garrabos, and G. Zalczer, Phys. Rev. Lett. 45, 403 (1980).

[4]The analogous parameter for the Rayleigh line is $(c_p/T)^{1/2}X^T/D_T k^2$ [cf. Eq. (5.2)].

[5]These assignments can be justified by iterating the equations for $M_{\alpha\rho}(\vec{R},\vec{q},\omega\approx O(q^2))$ and $D_{\alpha\beta}(\vec{R},\vec{q})$ about the equilibrium solution in powers of X^T.

[6]One might wonder whether the right-hand side of Eq. (2.2), which is of $O(X^T)$ is sufficiently accurate for the purpose of this paper, where terms of higher than first order in X^T are considered. Examining the derivation of the equations for the $D_{\alpha\beta}$ given in I, one sees that terms of relative order lX^T have been neglected on the right-hand side of Eq. (2.2). Since $l\,|X^T|\approx$

$$\frac{\Gamma_s}{c}|X^T|\approx\frac{\Gamma_s}{c}q\cdot\frac{|X^T|}{q}\ll 1\ ,$$

this approximation is justified.

[7]M. Ernst and J. R. Dorfman, J. Stat. Phys. 12, 311 (1975).

[8]In Ref. 20 of paper II it was remarked that the shape of the σ-Brillouin line was not determined by $M_{\sigma\rho}$ alone but by $M_{\sigma\rho}(\omega\approx\sigma ck)$, $M_{-\sigma\rho}(\omega\approx\sigma ck)$, and $M_{H\rho}(\omega\approx\sigma ck)$. However, the shape of the central line when $cX^T/\Gamma_s q^2\approx 1$ and $\Gamma_s q/c\ll 1$ is completely determined by $M_{H\rho}(\omega\approx 0)$ alone. To see this, one must use Eqs. (II. B1b), (II. B.3a), and (II. B3b), and see that all $R_{ab}^{(i)}$ are at least of $O(q^0)$. From these equations one can then see that all the terms on the right-hand side of Eq. (II. B1b) are at most of relative order $|X^T|/q\ll 1$ compared to $M_{H\rho,0}$. Since we are interested only in terms of relative order $O(X^T/q^2)$, these contributions can be neglected. Similar considerations can be used for the higher iterates of Eq. (II.B1b).

[9]In the experiment of Beysens *et al.*, $k\approx 2000$ cm^{-1}, $|\vec{\nabla}T|=75$ K cm, $T=313$ K, and $L\approx 0.02$ cm, so $kL=40$ and $L\,|X^T|=4.8\times 10^{-3}$.

[10]Actually, the iterated solution is asymptotic rather than convergent for any nonzero value of $cX^T/\Gamma_s q^2$ (see Appendix B).

[11]This is equivalent to assuming that all R_x dependence is through the hydrodynamic variables.

[12]For example, if $\psi/2=1°$, $\sin^2\theta=3\times 10^{-4}$.

[13]Equation (4.9) is exact if the sound velocity does not depend on temperature over the range of interest, i.e., when $m_3=0$. For H_2O, this a good approximation.

[14]T. R. Kirkpatrick and E. G. D. Cohen, Phys. Lett. 78A, 350 (1980).

[15]*Handbook of Mathematical Functions*, edited by M. Abramowitz and L. Stegun (National Bureau of Standards, Washington, D.C., 1964).

[16]These expansions break down if $1-(1/|a|)=n$ for $n=(0,1,2,\ldots)$, but in that case a different expansion can be used, cf. Dingle, Ref. 17.

[17]R. Dingle, *Asymptotic Expansions* (Academic, New York, 1973).

[18]See, for example, D. Pohl, S. Schwarz, and V. Irniger, Phys. Lett. 31, 32 (1973); D. Pohl and V. Irniger, Phys. Rev. Lett. 36, 480 (1976).

[19]T. R. Kirkpatrick and E. G. D. Cohen (unpublished).

[20]G. Satten and D. Ronis, Phys. Rev. A 26, 940 (1982).

[21]M. Ernst and J. R. Dorfman, Physica (Utrecht) 61, 157 (1972).

[22]Actually, Ernst and Dorfman (Ref. 21) considered the special case of hard-sphere molecules. We remark, however, that Eq. (C4) below can be shown to be valid for general short-ranged, repulsive interparticle potentials (Ref. 23).

[23]M. H. Ernst and E. G. D. Cohen, J. Stat. Phys. 25, 153 (1981).

[24]J. R. Dorfman and E. G. D. Cohen, Phys. Rev. A 6, 786 (1972).

[25]A similar discussion can be given for D_{vH}, important for the Rayleigh line.

[26]Strictly speaking, we should consider only the region $q_0<q<\sigma^{-1}$, since we have consistently neglected phenomena that occur on the length scale of the range of the intermolecular forces.

[27]See, for example, J. R. Dorfman and E. G. D. Cohen, J. Math. Phys. 8, 282 (1967).

[28]Y. Kan and J. R. Dorfman, Phys. Rev. A 16, 2447 (1977).